PREPARATION AND CHARACTERIZATION OF BIOPOLYMERIC NERVE GUIDES

BİYOPOLİMERİK SİNİR KILAVUZLARININ HAZIRLANMASI VE KARAKTERİZASYONU

YASEMİN BAYSAL

Submitted to Institute of Science of
Hacettepe University
as a partial fullfilment to the Requirements
for the degree of
DOCTORATE OF SCIENCE
in
CHEMİSTRY

2008

To the Institute for Graduate Studies in Pure and Applied Sciences,
This study has been accepted as a THESIS of DOCTORATE of SCIENCE in BIOCHEMISTRY by our examining committee.

Head :…….

Prof. Dr. Emir B. Denkbaş

Member :……

Prof. Dr. Adil Denizli

Member :……..

Assoc. Prof. Dr. Mehmet Ali Ergün

Member :……..

Assoc. Prof. Dr. Y. Çetin Kocaefe

Member :……..

Assoc. Prof. Dr. Handan Yavuz

APPROVEMENT
This thesis has been accepted on 17/06/2008 by the above mentioned examining committee members appointed through the Broads of the Directors of the Institute for Graduate Studies in Pure and Applied Sciences.

…../06/2008

Prof.Dr. Erdem YAZGAN
Director of the Institute for Graduate
Studies in Pure and Applied Sciences

BİYOPOLİMERİK SİNİR KILAVUZLARININ HAZIRLANMASI VE KARAKTERİZASYONU

Yasemin BAYSAL

ÖZ

Kitosan kaplı kalsiyum aljinat yapı iskeleti, sinir kılavuzlarına aday olarak hazırlanmıştır. Sunulan çalışmada, doğrusal kanallara sahip sinir kılavuzu yapı iskeletleri dondurup kurutma yöntemiyle hazırlanmıştır. Hazırlanan bu yapı iskeletleri mikron yapısı, su tutma kapasitesi, geçirgenlik, mekanik özellik, *in vitro* degradasyon ve biyouyumluluk testlerine göre karakterize edilmiştir. Işık mikroskobundan alınan görüntülerle, yapı iskeletinin gözenek çapları Image-Pro Express programı kullanılarak ölçülmüştür. Gözenek çapları, sodyum aljinat konsantrasyonuna bağlı olarak 29 μm ile 99 μm aralığında değişim göstermektedir. Yapı iskeletlerinin su tutma kapasitesi gravimetrik ölçümlerle belirlenmiştir. Su tutma kapasitesi %500 ile %2000 arasında, sodyum aljinat konsantrasyonu, $CaCl_2.2H_2O$ ve kitosan konsantrasyonuna bağlı olarak değişim göstermektedir. Yapı iskeletlerinin degradasyon profilleri 37^0C'de NaN_3 içeren fosfat tamponu içinde 13 hafta boyunca, kültür ortamında 5 gün boyunca değerlendirilmiştir. Degradasyon süresince, yapı iskeletlerinde fosfat tamponunda %33'luk, kültür ortamında %25'lik kütle kayıpları olmuştur. Kitosan kaplı kalsiyum aljinat yapı iskeletlerinin, molekül ağırlıkları 180-66000 Da aralığında değişim gösteren karbonhidrat ve protein moleküllerine karşı geçirgenliği optik yoğunluk ölçümleriyle belirlenmiştir. Bu çalışmanın sonucunda; yapı iskeletlerinin HSA ve glikoz moleküllerine karşı geçirgen olduğu tespit edilmiştir. Kuru ve yaş yapı iskeletlerinin dikim esnasında ve ameliyat sonrasında yapısında bir değişiklik olup-olmayacağını belirlemek amacıyla mekanik dayanıklılık testleri yapılmıştır. Hidratasyona uğramış yapı iskeletlerinin fizyolojik koşullarda, yumuşak ve esnek olduğu bu testlerle belirlenmiştir. Son olarak yapı iskeletlerinin kan uyumluluk ve biyouyumluluk testleri yapıldı. *In vitro* kan uyumluluk, hücre yapışma ve MTT test sonuçları, kitosan kaplı kalsiyum aljinat yapı iskeletlerinin herhangi bir sitotoksik etkiye sahip olmadığını göstermiştir.

Anahtar kelimeler: Aljinat, Kitosan, Yapı iskeleti, Sinir Kılavuzları, Sinir Yenilenmesi, Hücre Kültürü.

Danışman: Prof. Dr. Emir Baki Denkbaş, Hacettepe Üniversitesi, Kimya Bölümü, Biyokimya AD.

PREPARATION AND CHARACTERIZATION OF BIOPOLYMERIC NERVE GUIDES

Yasemin BAYSAL

Abstract

Chitosan coated calcium alginate scaffold has been evaluated as candidate materials used as nerve guide. A novel procedure was developed by using freeze-dry processing to create nerve guidance scaffolds, with uniaxial linear pores. These scaffolds were characterized using microstructure, water uptake, permeability, mechanic strength, *in vitro* degradation and biocompatibility studies. Pore size of the scaffolds were measured by Image-Pro Express software (MediaCybernetics, USA). Scaffolds' pore size changed with changing sodium alginate concentration between 29 μm to 99 μm. Water uptake capacity of the scaffolds was determined using gravimetric measurement. The most effective parameters on the water uptake behaviour of chitosan coated calcium alginate scaffolds were selected as sodium alginate, $CaCl_2.2H_2O$ and chitosan concentrations. Water uptake ratios between 500% to 2000% varied depending on these parameters. We examined the degradation profile of scaffolds certain periods of 13 weeks in PBS with NaN_3 at 37^0C and 5 days in culture medium at 37^0C. The mass loss of the scaffolds was about 33% in PBS and about 25% in culture medium at the end of degradation periods. The permeability of different molecules like carbohydrate and protein ranging from molecular weight 180–66,000 Da across the chitosan coated calcium alginate scaffolds were studied with optical density measurement. HSA and glucose molecules easily diffuse across the scaffolds. The mechanical strength of the dry and wet scaffolds was studied to ensure that the scaffolds could withstand suturing and remain intact after surgery. The hydrated scaffolds were soft and flexible and stable under physiological conditions. Blood compatibility and biocompatibility studies of the scaffolds were performed. *In vitro* haemocompatibility tests, cell attachment studies and MTT assay results show that, the chitosan coated calcium alginate scaffold doesn't have any cytotoxic effect.

Key words: Alginate, Chitosan, Scaffold, Nerve Guides, Nerve Regeneration, Cell Culture.

Advisor: Prof. Dr. Emir B. DENKBAS, Hacettepe University, Department of Chemistry, Biochemistry Division.

ACKNOWLEDGEMENT

I am very greatly obliged and indebted to Prof. Dr. Emir Baki Denkbaş, my supervisor, for his valuable guidance, professional advice, constrictive critism and suggestion during my research.

Special thanks to Prof. Dr. Adil Denizli and Assoc. Prof. Dr. Handan Yavuz for their suggestions throughout my Ph.D. Study.

I am very greatful to Assoc. Prof. Dr. Çetin Kocaefe for their supports during my thesis..

I wish to thank all my friends Ayla Şener, Cem Bayram, Tamer Çırak, Sedat Odabaş, Murat Demirbilek, Doğa Kavaz, Burcu Aslan, Lokman Uzun, Nilay Bereli, Müge Andaç and others for their help in laboratory, for their collaborating asssisting and providing me a pleasant atmosphere to work in.

I am very greatful to Süleyman Sabuncuoğlu *for their supports during my thesis..*

Also I would like to thank all colleagues in Chemistry Department.

Special thanks to my husband, Mehmet Yasin Baysal, for his support and encouragement during my Ph. D. Studies. Thanks a lot for all things.

Finally, I am very much indepted to my family for their support and encouragement during my Ph.D. studies.

INDEX

Page No

FIGURE INDEX

Page No

TABLE INDEX **Page No**

ABBREVIATIONS

SEM	Scanning Electron Microscopy
MMW	Medium Molecular Weight
FTIR	Fourier Transform Infra-red Spectroscopy
h	Hour
min.	Minute
APTT	Activated Partial Thromboplastin Time
PT	Prothrombin Time
DA	Degree of acetylation
MTT	3-(4,5-dimethylthiazol-2-yl)-2,5-diphenyltetrazolium bromide
MW	Molecular Weight
PBS	Phosphate Buffer Saline

1. INTRODUCTION

Peripheral nerve injuries can result from travma, mechanical, thermal, chemical reasons or pathological etiology. Failure to restore these damaged nerves can lead to the loss of muscle function, impaired sensation and painful neuropathies. A greater awareness and understanding of the nerve ultrastucture, as well as the underlying mechanisms of the regenerative process and those factors detrimental to nerve regeneration, will assist in the successful repair of nerve injury. When nerves are cut or torn apart with trauma, they need to be reattached so that recovery can occur. Reconstruction of nerve continuity can be performed with direct repair. This is performed when the 2 ends of the nerve are directly coapted. This should be performed without tension. If the repair cannot be performed without tension, nerve grafting should be performed. If the adjacent joint must be flexed or extended to permit coaptation of the distal and proximal ends of the nerve, a nerve graft should be used. (With wrist flexion, the median nerve can be directly repaired; if it is under tension with wrist in neutral position, a nerve graft should be used). Several disadvantages of nerve grafts have led to the development of new techniques during the last decades. Nerve conduits for reconstruction of damaged nerves have been developed, such as the use of vessels (regular veins, inside-out veins and arteries), synthetic materials (silicone and polyglycolic acid), biological conduits (collagen), and muscle conduits (Tang et al., 1995; Chen et al., 1994; Kim et al., 1993; Keeley et al., 1991; Wang et al., 1995). Gaps up to 8 cm can be bridged with nerve guides (Zhang et al., 2002; Matsumoto et al., 2000). Strategies to improve healing of damaged nerves include the application of specialized nerve guides, which hold the promise for allowing reanastomosis of the severed or damaged fibers (Berger et al., 1994; Wang et al., 1999). Nowadays, artificial biodegradable nerve guides are widely studied for bridging peripheral nerve defects. The use of biodegradable nerve guides can be a practical tool to provide neutrophic and/or cellular support while simultaneously guiding axonal regeneration. Studies have demonstrated that the use of a slowly degradable polymeric nerve guide can improve the nature and rate of nerve regeneration across a short gap in small nerves (den Dunnen et al., 2000; Matsumoto et al., 2000; Evans et al., 1999; Aldini et al., 1996). Also non-degradable nerve guides were applied but their main disadvantage being that the material remains in situ as a foreign body, potentially causing a chronic reaction with

excessive scar tissue formation (IJkema-Paassen et al., 2004). This might result in constriction of the regenerating nerve, ultimately hazarding the recovery of nerve function (e.g. secondary nerve impairment) (Merle et al., 1989; Mackinnon et al., 1984). Biodegradable nerve guides therefore promise to be a successful alternative, their aim being to direct the outgrowing nerve fibres towards the distal nerve stump, whilst preventing neuroma formation and ingrowth of fibrous tissue into the nerve gap (IJkema-Paassen et al., 2004). As reviewed by Fields, et al., 1989, a variety of materials have been used to prepare nerve guides, ranging from biological materials, metals, silicone rubbers, synthetic materials and bioresorbable materials. The ideal nerve guide should possess the following characteristics: (a) inert and biocompatible; (b) thin, flexible and of appropriate mechanical properties; (c) translucent; (d) bioresorbable; (e) able to inhibit pathological processes and (f) beneficial to healing and regeneration (Fields et al., 1989). The vast majority of the referenced literature describe the use of nerve guides to enhance nerve regeneration without the addition of other components. In this sense, the nerve guide is acting as a physical barrier to aid in the directionality of nerve growth (Verreck et al., 2004). Only a few applications can be found where a biologically active material is incorporated into the polymeric matrix of the guide to enhance neuronal growth (Xu et al., 2002; Xu et al., 2003; Rosner et al., 2003).

Numerous natural and synthetic polymers, including poly-(α-hydroxyacids), collagen, fibronectin, and hyaluronic acid, have been used as scaffolds or within scaffolds for peripheral and central nerve regeneration, and have been reviewed in detail (Schmidt et al., 1993; Geller et al., 2002). Many of the fabrication technologies for these polymers are based on particulate-leaching techniques, heat compression, and extrusion (Hadlock et al., 1999; Lin et al., 1993). However, the harsh operating conditions of these processes can limit the incorporation of bioactive proteins and cells, and residual amounts of the chemical solvents required may cause toxicity in vivo (Stokols et al., 2004). Freeze/dry processing is an alternative method for producing porous scaffolds that does not require additional chemicals, relying instead on the water already present in hydrogels to form ice crystals that can be sublimated from the polymer, creating a particular micro-architecture (Stokols et al, 2004). Because the direction of growth and size of the ice crystals are a function of the

temperature gradient, linear, radial, and/or random pore directions and sizes can be produced with this methodology (Madihally et al., 1999).

In the present study; alginate and chitosan biopolymers were selected to prepare nerve guides. The biopolymeric nerve guides were developed by using freeze-dry processing to create uniaxial linear pores. Alginate and chitosan are a class of biodegradable polymers with a variety of attractive properties (i.e biocompatible, abudance in source, low price and non-toxic). Alginate, a natural polysaccharide found in brown algae, is a linear 1,4 linked copolymer of β-D-mannuronic acid (M) and α-L-gulunoric acid (G). Sodium alginate scaffolds were prepared by freeze/dry processing. After that we placed the sodium alginate scaffold into $CaCl_2.2H_2O$ solution which has different concentrations. We used chitosan to coat the calcium alginate scaffolds to improve biocompatibility and mechanical strength of the calcium alginate scaffolds. Chitosan and alginate are polyelectrolyte polymers and they have opposite charges; sodium alginate which has a carboxyl group (COO^-) contains a negative charge, while chitosan which has an ammonium group (NH_3^+) contains a positive one. They are formed polyionic complex through electrostatic interaction. Chitosan is a deacetylated derivative of chitin, a naturally occurring polymer. It is widely studied in pharmaceutical and biomedical fields because of its biodegradability, its biocompatibility and its interesting structural properties (presence of amino and hydroxyl groups) (Ric`cardo and Muzzarelli, 1977; Denuziere, 1996; Sharma and Rao, 1997; Hirano, 1999; Shepherd et al., 1997).

After fabrication of chitosan coated alginate scaffolds, these scaffolds were characterized for microstructure, water uptake, permeability, mechanical strength, in vitro degradation, *in vitro* haemocompatibility tests and biocompatibility (cell attachment study and MTT assay).

2. GENERAL INFORMATION

2.1. Nervous Systems

Multicellular animals must monitor and maintain a constant internal environment as well as monitor and respond to an external environment. In many animals, these two functions are coordinated by two integrated and coordinated organ systems: the nervous system and the endocrine system.

Three basic functions are performed by nervous systems:

1. Receive sensory input from internal and external environments
2. Integrate the input
3. Respond to stimuli

2.1.1. Sensory input

Receptors are parts of the nervous system that sense changes in the internal or external environments. Sensory input can be in many forms, including pressure, taste, sound, light, blood pH, or hormone levels, that are converted to a signal and sent to the brain or spinal cord.

2.1.2. Integration and output

In the sensory centers of the brain or in the spinal cord, the barrage of input is integrated and a response is generated. The response, a motor output, is a signal transmitted to organs than can convert the signal into some form of action, such as movement, changes in heart rate, release of hormones, etc.

2.1.3. Endocrine systems

Some animals have a second control system, the endocrine system. The nervous system coordinates rapid responses to external stimuli. The endocrine system controls slower, longer lasting responses to internal stimuli. Activity of both systems is integrated.

2.2. Divisions of the Nervous System

The nervous system monitors and controls almost every organ system through a series of positive and negative feedback loops.The Central Nervous System (CNS) includes the brain and spinal cord. The Peripheral Nervous System (PNS) connects the CNS to other parts of the body, and is composed of nerves (bundles of neurons).

Not all animals have highly specialized nervous systems. Those with simple systems tend to be either small and very mobile or large and immobile. Large, mobile animals have highly developed nervous systems: the evolution of nervous systems must have been an important adaptation in the evolution of body size and mobility.

2.2.1. Peripheral nervous system

The Peripheral Nervous System (PNS) contains only nerves and connects the brain and spinal cord (CNS) to the rest of the body. The axons and dendrites are surrounded by a white myelin sheath. Cell bodies are in the central nervous system (CNS) or ganglia. Ganglia are collections of nerve cell bodies. Cranial nerves in the PNS take impulses to and from the brain (CNS). Spinal nerves take impulses to and away from the spinal cord. There are two major subdivisions of the PNS motor pathways: the somatic and the autonomic.

Two main components of the PNS:

1. sensory (afferent) pathways that provide input from the body into the CNS.
2. motor (efferent) pathways that carry signals to muscles and glands (effectors).

Most sensory input carried in the PNS remains below the level of conscious awareness. Input that does reach the conscious level contributes to perception of our external environment.

2.2.2. Somatic nervous system

The Somatic Nervous System (SNS) includes all nerves controlling the muscular system and external sensory receptors. External sense organs (including skin) are receptors. Muscle fibers and gland cells are effectors. The reflex arc is an automatic, involuntary reaction to a stimulus. When the doctor taps your knee with the rubber

hammer, she/he is testing your reflex (or knee-jerk). The reaction to the stimulus is involuntary, with the CNS being informed but not consciously controlling the response. Examples of reflex arcs include balance, the blinking reflex, and the stretch reflex.

Sensory input from the PNS is processed by the CNS and responses are sent by the PNS from the CNS to the organs of the body.

Motor neurons of the somatic system are distinct from those of the autonomic system. Inhibitory signals, cannot be sent through the motor neurons of the somatic system.

2.2.3. Autonomic nervous system

The Autonomic Nervous System is that part of PNS consisting of motor neurons that control internal organs. It has two subsystems. The autonomic system controls muscles in the heart, the smooth muscle in internal organs such as the intestine, bladder, and uterus. The Sympathetic Nervous System is involved in the fight or flight response. The Parasympathetic Nervous System is involved in relaxation. Each of these subsystems operates in the reverse of the other (antagonism). Both systems innervate the same organs and act in opposition to maintain homeostasis. For example: when you are scared the sympathetic system causes your heart to beat faster; the parasympathetic system reverses this effect.

Motor neurons in this system do not reach their targets directly (as do those in the somatic system) but rather connect to a secondary motor neuron which in turn innervates the target organ.

2.2.4. Central nervous system

The Central Nervous System (CNS) is composed of the brain and spinal cord. The CNS is surrounded by bone-skull and vertebrae. Fluid and tissue also insulate the brain and spinal cord.

The brain is composed of three parts: the cerebrum (seat of consciousness), the cerebellum, and the medulla oblongata (these latter two are "part of the unconscious brain").

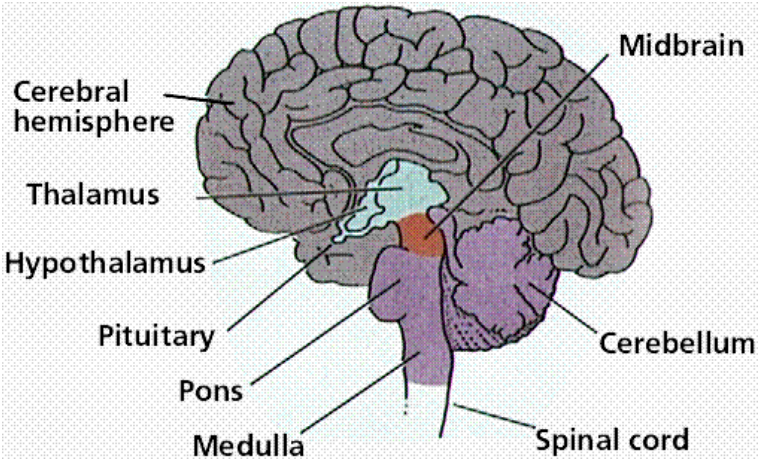

Figure 2.1. Parts of the brain as seen from the middle of the brain.

The medulla oblongata is closest to the spinal cord, and is involved with the regulation of heartbeat, breathing, vasoconstriction (blood pressure), and reflex centers for vomiting, coughing, sneezing, swallowing, and hiccuping. The hypothalamus regulates homeostasis. It has regulatory areas for thirst, hunger, body temperature, water balance, and blood pressure, and links the Nervous System to the Endocrine System. The midbrain and pons are also part of the unconscious brain. The thalamus serves as a central relay point for incoming nervous messages.

The cerebellum is the second largest part of the brain, after the cerebrum. It functions for muscle coordination and maintains normal muscle tone and posture. The cerebellum coordinates balance.

The conscious brain includes the cerebral hemispheres, which are separated by the *corpus callosum*. In reptiles, birds, and mammals, the cerebrum coordinates sensory data and motor functions. The cerebrum governs intelligence and reasoning, learning and memory. While the cause of memory is not yet definitely known, studies on slugs indicate learning is accompanied by a synapse decrease. Within the cell, learning involves change in gene regulation and increased ability to secrete transmitters.

2.2.4.1. The brain stem and midbrain

The brain stem is the smallest and from an evolutionary viewpoint, the oldest and most primitive part of the brain. The brain stem is continuous with the spinal cord, and is composed of the parts of the hindbrain and midbrain. The medulla oblongata and pons control heart rate, constriction of blood vessels, digestion and respiration.

The midbrain consists of connections between the hindbrain and forebrain. Mammals use this part of the brain only for eye reflexes.

2.2.4.2. The spinal cord

The spinal cord runs along the dorsal side of the body and links the brain to the rest of the body. Vertebrates have their spinal cords encased in a series of (usually) bony vertebrae that comprise the vertebral column.

The gray matter of the spinal cord consists mostly of cell bodies and dendrites. The surrounding white matter is made up of bundles of interneuronal axons (tracts). Some tracts are ascending (carrying messages to the brain), others are descending (carrying messages from the brain). The spinal cord is also involved in reflexes that do not immediately involve the brain.

2.3. Nerve Degeneration

Definition: Loss of functional activity and trophic degeneration of nerve axons and their terminal arborizations following the destruction of their cells of origin or interruption of their continuity with these cells. The pathology is characteristic of neurodegenerative diseases. Often the process of nerve degeneration is studied in research on neuroanatomical localization and correlation of the neurophysiology of neural pathways.

2.3.1. Wallerian degeneration

Wallerian Degeneration results from axonal injury, and occurs in axons in both the Peripheral nervous system (PNS) and Central Nervous System (CNS). It occurs at the distal stump of the site of injury and usually begins within 24 hours of a lesion. Prior to degeneration distal axon stumps tend to remain electrically excitable . After

injury, the axonal skeleton disintegrates and the axonal membrane breaks apart. The axonal degeneration is followed by degradation of the myelin sheath and macrophage infiltration. The macrophages, accompanied with Schwann cells serve to clear the debris from the degeneration (Waller, 1850; Coleman et al., 1998).

2.3.1.1. History

Wallerian degeneration is named after Augustus Volney Waller. Waller conducted his experiment in 1850, on frogs by severing their glossopharyngeal and hypoglossal nerves. He then observed the distal nerves from the site of injury, which were separated from their cell bodies in the brain stem (Waller, 1850). Waller described the disintegration of myelin, which he referred to as "medulla", into separate particles of various sizes. The degenerated axons formed droplets that could be stained, thus allowing studies of the course of individual nerve fibres.

2.3.2. Axonal degeneration

Although most injury responses include a calcium influx signaling to promote resealing of severed parts, axonal injuries initially lead to acute axonal degeneration (AAD), which is rapid separation of the proximal and distal ends within 30 minutes of injury (Kerschensteiner et al., 2005). Degeneration follows with swelling of the axolemma, and eventually leads to bead like formation. The process takes about roughly 24 hrs in the PNS, and longer in the CNS. The signaling pathways leading to axolemma degeneration are currently unknown. However, research has shown that this AAD process is calcium – independent (Vargas et al., 2007).

Granular disintegration of the axonal cytoskeleton and inner organelles occurs after axolemma degradation. Early changes include accumalation of mitochondria in the paranodal regions at the site of injury. Endoplasmic reticulum degrades and mitochondria swell up and eventually disintegrate. The depolymerization of microtubules occurs and is soon followed by degradation of the neurofilaments and other cytoskeleton components. The disintegration is dependent on Ubiquitin and Calpain proteases (casued by influx of calcium ion), suggesting that axonal degeneration is an active process and not a passive one as previously misunderstood (Zimmerman et al., 1984). Thus the axon undergoes complete

fragmentation. The rate of degradation is dependent on the type of injury and also varies from PNS to CNS, being slower in CNS. Another factor that affects degradation rate includes axon diameter. Larger axons require longer time for cytoskeleton degradation and thus take a longer time to degenerate.

2.3.3. Myelin clearance

Myelin is a phospholipid membrane that wraps around axons to provide them with insulation. Its produced by Schwann cells in the PNS, and by Oligodendrocytes in the CNS. Myelin clearance is the next step in Wallerian degeneration following axonal degeneration. The cleaning up of myelin debris is different for PNS and CNS. PNS is much faster and efficient at clearing myelin debris in comparison to CNS, and Schwann cells are the primary cause of this difference. Another key aspect is the change in permeability of the blood-tissue barrier in the two systems. In PNS, the permeability increases throughout the distal stump, but the barrier disruption in CNS is limited to just the site of injury (Vargas et al., 2007).

2.3.4. Clearance in PNS

The response of Schwann cells to axonal injury is rapid. The time period of response is estimated to be prior to the onset of axonal degeneration. Neuregulins are believed to be responsible for the rapid activation. They activate ErbB2 receptors in the Schwann cell microvilli, which results in the activation of the mitogen-activated protein kinase (MAPK) (Guertin et al., 2005). Although MAPK activity is observed, the injury *sensing* mechanism of Schwann cells is yet to be fully understood. The *sensing* is followed by decreased synthesis of myelin lipids and eventually stops within 48 hrs. The myelin sheaths separate from the axons at the Schmidt-Lanterman incisures first and then rapidly deteriorate and shorten to form bead-like structures. Schwann cells continue to clear up the myelin debris by degrading their own myelin, phagocytose extracellular myelin and attract macrophages to myelin debris for phagocytosis (Vargas et al., 2007). However, the macrophages are not attracted to the region for the first few days; hence the Schwann cells take the major role in myelin cleaning until then.

Schwann Cells have been observed to recruit macrophages by release of cytokines and chemokines after *sensing* of axonal injury. The recruitment of macrophages helps improve the clearing rate of myelin debris. The resident macrophages present in the nerves release further chemokines and cytokines to attract further macrophages. The degenerating nerve also produce macrophage chemotactic molecules. Another source of macrophage recruitment factors is serum. Delayed macrophage recruitment was observed in B-cell deficient mice lacking serum anitbodies (Vargas et al., 2005). These signaling molecules together cause an influx of macrophages, which peaks during the third week after injury. While Schwann cells mediate the initial stage of myelin debris clean up, macrophages come in to finish the job. Macrophages are facilitated by opsonins, which label debris for removal. The 3 major groups found in serum include complement, pentraxins, and antibodies. However, only complement has shown to help in myelin debris phagocytosis (Dailey et al., 1998).

Murinson et al., (2005) observed that non-myelinated or myelinated Schwann cells in contact with an injured axon enter cell cycle thus leading to proliferation. Observed time duration for Schwann cell divisions where approximately 3 days after injury (Liu et al., 1995). Possible sources of proliferation signal are attributed to the ErbB2 receptors and the ErbB3 receptors. This proliferation could further enhance the myelin cleaning rates and plays an essential role in regeneration of axons observed in PNS. Schwann cells emit growth factors which attract new axonal sprouts growing from the proximal stump after complete degeneration of the injured distal stump. This leads to possible reinnervation of the target cell or organ. However, the reinnervation is not necessarily perfect as possible misleading occurs during reinnervation of the proximal axons to target cells.

2.3.5. Clearance in CNS

In comparison to Schwann cells, Oligodendrocytes require axon signals to survive. In their developmental stages, oligodendrocytes that failed to make contact to axon and receive any axon signals under went apoptosis (Barres et al., 1993). Experiments in wallerian degeneration have shown that upon injury oligodendrocytes either under go programmed cell death or enter a state of rest. Therefore, unlike Schwann cells, oligodendrocytes fail to clean up the myelin sheaths and their debris. In experiments

conducted on rats (Ludwin, 1990), myelin sheaths were found for up to 22 months. Therefore, CNS rates of myelin sheath clearance are very slow and could possibly be the cause for hindrance in the regeneration capabilities of the CNS axons as no growth factors are available to attract the proximal axons. Another feature that results eventually is Glial scar formation. This further hinders chances for regeneration and reinnervation.

Oligodendrocytes fail to recruit macrophages for debris removal. Macrophage entry in general into CNS site of injury is very slow. In contrast to PNS, Microglia play a vital role in CNS wallerian degeneration. However, their recruitment is slower in comparison to macrophage recruitment in PNS by approximately 3 days. Further, microglia might be activated but hypertrophy, and fail to transform into fully phagocytic cells. Those microglia that do transform, clear out the debris effectively. Differentiating phagocytic microglia can be accomplished by testing for expression of Major histocompatibility complex (MHC) class I and II during wallerian degeneration (Koshinaga et al., 1995). The rate of clearance is very slow among microglia in comparison to macrophages. Possible source for variations in clearance rates could include lack of opsonin activity around microglia, and the lack of increased permeability in the blood-brain barrier. The decreased permeability could further hinder macrophage infiltration to the site of injury (Vargas et al., 2007).

These findings have suggested that the delay in wallerian degeneration in CNS in comparison to PNS is caused not due to a delay in axonal degeneration, but rather is due to the difference in clearance rates of myelin in CNS and PNS (George et al., 1994).

2.4. Regeneration

Regeneration follows degeneration. Regeneration is rapid in PNS, and might need some grafts for appropriate reinnervation. It is supported by Schwann cells through growth factors release. CNS regeneration is much slower, and is almost absent in most species. The primary cause for this could be the delay in clearing up myelin debris. Myelin debris, present in CNS or PNS, contains several inhibitory factors. The elongated presence of myelin debris in CNS could possibly hinder the regeneration (He et al., 2004). An experiment conducted on Newt, an animal with fast CNS axon

regeneration capabilities, found that wallerian degeneration of an optic nerve injury took upto 10 to 14 days on average, further suggesting that slow clearance inhibits regeneration (Turner et al., 1976).

2.4.1. Schwann cells and endoneural fibroblasts in PNS

In healthy nerves, Nerve growth factor (NGF) is procuded in very small amounts. However, upon injury, NGF mRNA expression increases by five to seven fold within a period of 14 days. Nerve fibroblasts and Schwann cells play an important role in increased expression of NGF mRNA (Heumann et al., 1987). Macrophages also stimulate Schwann cells and fibroblasts to produce NGF via macrophage-derived interleukin-1 (Lindholm et al., 1988). Other neurotrophic molecules produced by Schwann cells and fibroblasts together include Brain-derived neurotrophic factor, Glial cell line-derived neurotrophic factor, Ciliary neurotrophic factor, Leukemia inhibitory factor, Insulin-like growth factor, and Fibroblast growth factor. These factors together create a favorable environment for axonal growth and regeneration (Vargas et al., 2007). Apart from growth factors, Schwann cells also provide structural guidance to further enhance regeneration. During their proliferation phase, Schwann cells begin to form a line of cells called *Bands of Bunger* within the basal laminar tube. Axons have been observed to regenerate in close association to these cells (Thomas et al., 1974) Schwann cells upregulate the production of cell surface adhesion molecule ninjurin further promoting growth (Araki et al., 1996). These lines of cell guide the axon regeneration in proper direction. The possible source of error that could result from this is possible mismatching of the target cells as discussed earlier.

Due to lack of such favorable promoting factors in CNS, regeneration is stunted in CNS.

2.5. Nerve Repair

When nerves are cut or torn apart with trauma, they need to be reattached so that recovery can occur. Using a microscope, the nerve ends are re-attached with very fine sutures, which are difficult to see without the microscope. The nerve and its sub-compartments (fascicles) are attached in proper orientation based on anatomical

features. Sometimes a dab of fibrin glue is also used to seal this repair. It is important that there is no tension.

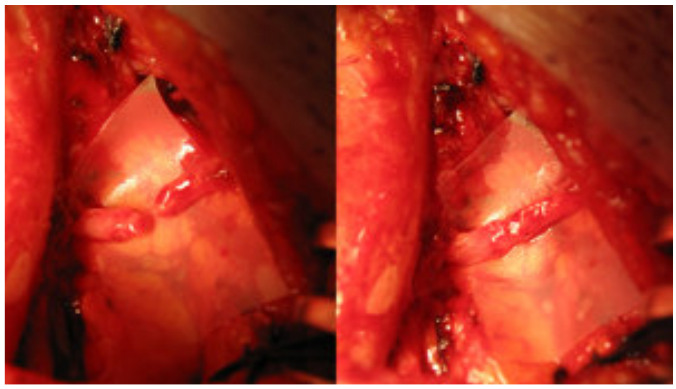

Figure 2.2. Direct nerve repair before (rigth) and after (left) suture.

2.5.1. Nerve grafting

If the ends of a cut or damaged nerve do not reach, then a nerve graft needs to be placed in between. This is often the case with stretch injuries or when there is extensive scar in the nerve that has to be removed. The nerve graft is taken from your leg, usually the sural nerve, which is a sensory nerve behind the calf. In removing this nerve you will have a patch of numbness on the side of your foot, which mostly resolves in 6-12 months. The nerve fibers in the graft tissue quickly dissolve, but the channels for new nerves to regenerate, as well as required growth factors still remain. Therefore once connected, the injured nerve fascicles grow through this graft.

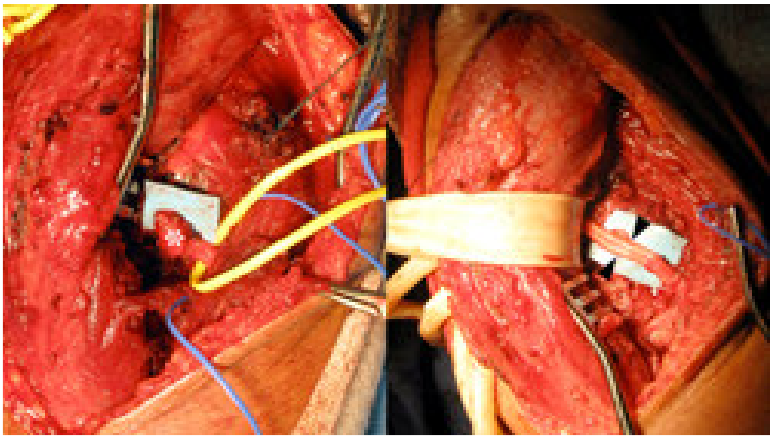

Figure 2.3. Nerve grafting image.

The grafts are sutured to the ends of the injured nerve with fine sutures using a microscope. Depending on the size of the injured nerve, multiple grafts may be required to repair the nerve. Longer the nerve graft, less likely that it will be successful.

In figure 2.3., patient had a disruption of their posterior interosseous nerve. The distal nerve stump (left, asterisk) was removed and the nerve was repaired with two sural nerve grafts (rigth, arrowheads). The proximal graft connection (not shown) is on the other side of the extensor muscle mass (rubber loop).

2.5.2. End-to-Side repair

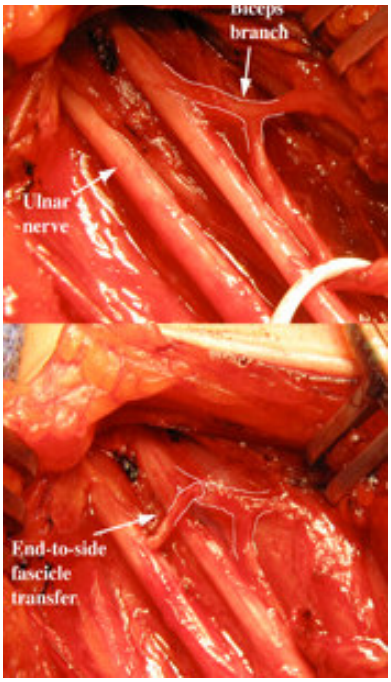

This is a variation of the nerve transfer. If the injured nerve is partially functional, or has the potential to recover, you do not want to cut it so that a full nerve transfer can be performed. Instead you make a window in the outer nerve sheath and attach the nerve transfer to the side of the nerve.

In general, some partial injury to the recipient nerve occurs, and this allows for the end-to-side transfer to regenerate down the recipient nerve. More fascicular injury to the recipient nerve leads to a greater amount of regeneration from the transferred nerve.

This procedure is often used to supplement other nerve repair techniques.

Figure 2.4. End to side repair image.

In figure 2.4., patient had partial function of their biceps motor branch (left). To supplement this function, an end-to-side nerve transfer was performed using a fascicle from the nearby ulnar nerve (rigth).

2.5.3. Conduit nerve repair

When repairing sensory nerves, it often does not make sense to remove another sensory nerve from the leg as a source of graft. Therefore, in this situation, if a direct repair is not possible, small absorbable tubes are used instead.

In general, as long as the nerve gap is less than 2-3 cm, conduit repair works nearly as well as graft repair. An alternative is to use a vein conduit, which has a similar efficacy. Conduits are also used to wrap nerves to protect them from nearby scar tissue.

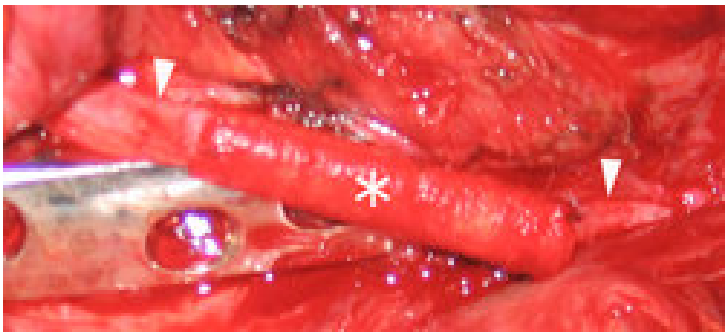

Figure 2.5. Nerve repairment by using conduit.

Synthetic nerve conduit (asterisk) used to repair a sensory branch from the radial nerve (proximal and distal nerve ends--arrowheads).

2.5.4. Nerve transfers

Example soft nerve transfers. Intercostal to musculocutaneous nerve transfer using three intercostal donors (left). Triceps branch to the anterior division of the axillary nerve transfer (middle). Medial pectoral nerve transfer to the axillary nerve (rigth). A nerve transfer is when a normal nerve is cut and subsequently attached to the distal end of an injured nerve, preferably as close as possible to the muscle. This is often performed when the proximal portion of the injured nerve is not available for direct or graft repair (e.g., when the injured nerve is pulled from the spinal cord during a brachial plexus injury). In select cases, a nerve transfer is recommended even when a graft repair is possible.

A normal donor nerve is selected so that the patient does not notice it being cut (e.g., from a muscle that has multiple branches, or from a muscle that shares function with other muscles). In general, the nerve receiving the transfer is more important than the donor. Even though the nerves are re-routed, brain plasticity allows for contraction to occur without difficulty in most patients.

Examples are listed below:

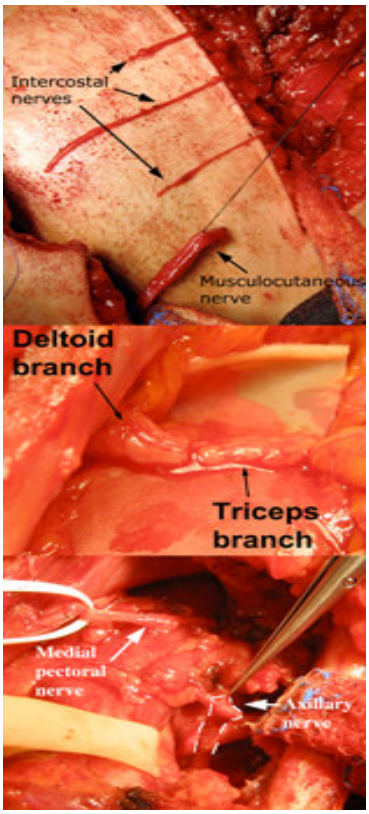

- Hypoglossal to facial
- Hypoglossal to spinal accessory
- Spinal accessory to suprascapular - anterior approach
- Spinal accessory to suprascapular - posterior approach
- Spinal accessory to musculocutaneous
- Medial pectoral to axillary
- Medial pectoral to musculocutaneous
- Thoracodorsal to axillary
- Thoracodorsal to musculocutaneous
- Triceps branch to axillary
- Intercostals to musculocutaneous
- Intercostals to long thoracic

Figure 2.6. Soft nerve transfer.

- Ulnar fascicle to biceps branch
- Median fascicle to brachialis branch
- Anterior interosseous to ulnar motor branch
- Femoral branch to gluteal nerve
- Femoral branch to hamstring branch
- Femoral branch to obturator
- Tibial branch to tibialis anterior

2.6. Nervous Tissue

Nervous tissue is composed of two main cell types: neurons and glial cells. Neurons transmit nerve messages. Glial cells are in direct contact with neurons and often surround them. The neuron is the functional unit of the nervous system. Humans have about 100 billion neurons in their brain alone! While variable in size and shape, all neurons have three parts. Dendrites receive information from another cell and

transmit the message to the cell body. The cell body contains the nucleus, mitochondria and other organelles typical of eukaryotic cells. The axon conducts messages away from the cell body.

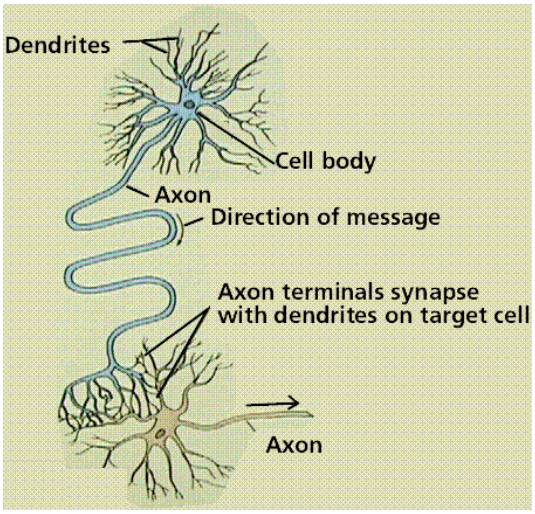

Figure 2.7. Structure of a neuron and the direction of nerve message transmission.

Three types of neurons occur. Sensory neurons typically have a long dendrite and short axon, and carry messages from sensory receptors to the central nervous system. Motor neurons have a long axon and short dendrites and transmit messages from the central nervous system to the muscles (or to glands). Interneurons are found only in the central nervous system where they connect neuron to neuron.

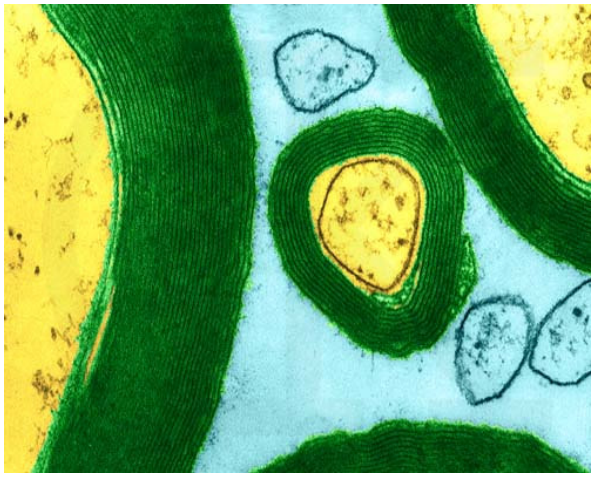

Figure 2.8. Cross section of **myelin sheaths** that surround **axons** (TEM x191,175).

Some axons are wrapped in a myelin sheath formed from the plasma membranes of specialized glial cells known as Schwann cells. Schwann cells serve as supportive, nutritive, and service facilities for neurons. The gap between Schwann cells is known as the node of Ranvier, and serves as points along the neuron for generating a signal. Signals jumping from node to node travel hundreds of times faster than signals traveling along the surface of the axon. This allows your brain to communicate with your toes in a few thousandths of a second.

2.6.1. The nerve message

The plasma membrane of neurons, like all other cells, has an unequal distribution of ions and electrical charges between the two sides of the membrane. The outside of the membrane has a positive charge, inside has a negative charge. This charge difference is a resting potential and is measured in millivolts. Passage of ions across the cell membrane passes the electrical charge along the cell. The voltage potential is -65mV (millivolts) of a cell at rest (resting potential). Resting potential results from differences between sodium and potassium positively charged ions and negatively charged ions in the cytoplasm. Sodium ions are more concentrated outside the membrane, while potassium ions are more concentrated inside the membrane. This imbalance is maintained by the active transport of ions to reset the membrane known as the sodium potassium pump. The sodium-potassium pump maintains this unequal concentration by actively transporting ions against their concentration gradients. Changed polarity of the membrane, the action potential, results in propagation of the nerve impulse along the membrane. An action potential is a temporary reversal of the electrical potential along the membrane for a few milliseconds. Sodium gates and potassium gates open in the membrane to allow their respective ions to cross. Sodium and potassium ions reverse positions by passing through membrane protein channel gates that can be opened or closed to control ion passage. Sodium crosses first. At the height of the membrane potential reversal, potassium channels open to allow potassium ions to pass to the outside of the membrane. Potassium crosses second, resulting in changed ionic distributions, which must be reset by the continuously running sodium-potassium pump. Eventually enough potassium ions pass to the outside to restore the membrane charges to those of the original resting

potential.The cell begins then to pump the ions back to their original sides of the membrane.

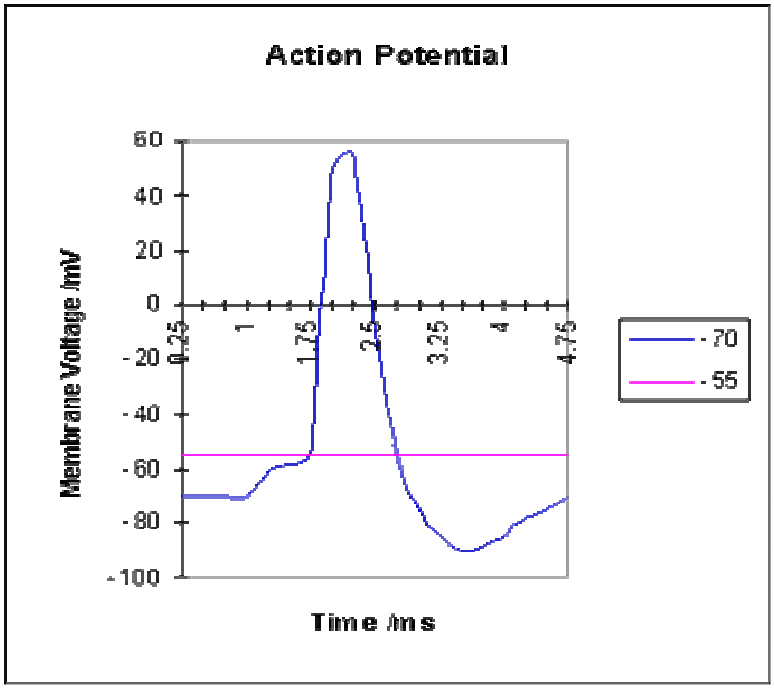

Figure 2.9. Transmission of an action potential.

The action potential begins at one spot on the membrane, but spreads to adjacent areas of the membrane, propagating the message along the length of the cell membrane. After passage of the action potential, there is a brief period, the refractory period, during which the membrane cannot be stimulated. This prevents the message from being transmitted backward along the membrane.

2.6.1.1. Steps in an action potential

1. At rest the outside of the membrane is more positive than the inside.
2. Sodium moves inside the cell causing an action potential, the influx of positive sodium ions makes the inside of the membrane more positive than the outside.
3. Potassium ions flow out of the cell, restoring the resting potential net charges.
4. Sodium ions are pumped out of the cell and potassium ions are pumped into the cell, restoring the original distribution of ions.

2.6.2. Synapses

The junction between a nerve cell and another cell is called a synapse. Messages travel within the neuron as an electrical action potential. The space between two cells is known as the synaptic cleft. To cross the synaptic cleft requires the actions of neurotransmitters. Neurotransmitters are stored in small synaptic vessicles clustered at the tip of the axon.

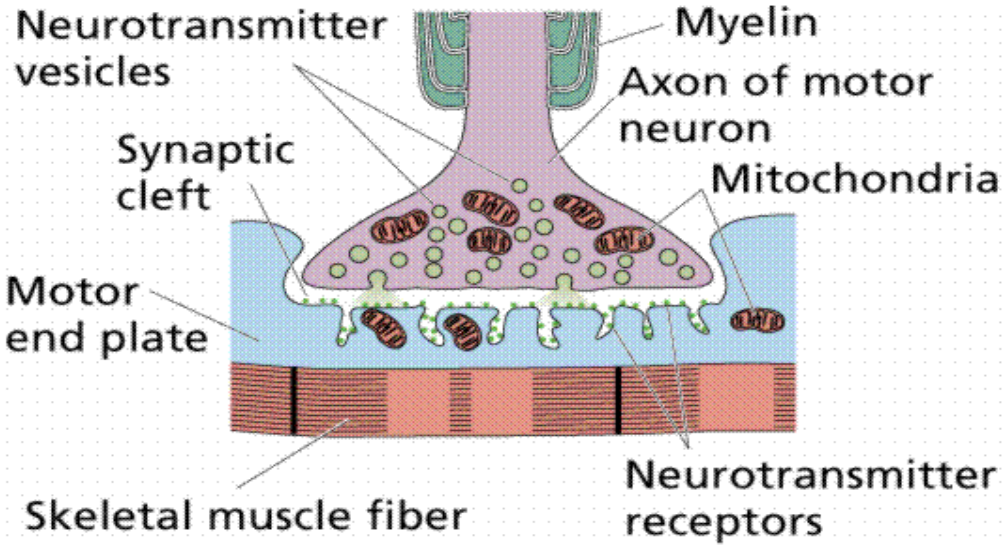

Figure 2.10. A synapse.

Arrival of the action potential causes some of the vesicles to move to the end of the axon and discharge their contents into the synaptic cleft. Released neurotransmitters diffuse across the cleft, and bind to receptors on the other cell's membrane, causing ion channels on that cell to open. Some neurotransmitters cause an action potential, others are inhibitory.

Neurotransmitters tend to be small molecules, some are even hormones. The time for neurotransmitter action is between 0.5 and 1 millisecond. Neurotransmitters are either destroyed by specific enzymes in the synaptic cleft, diffuse out of the cleft, or are reabsorbed by the cell. More than 30 organic molecules are thought to act as neurotransmitters. The neurotransmitters cross the cleft, binding to receptor molecules on the next cell, prompting transmission of the message along that cell's membrane. Acetylcholine is an example of a neurotransmitter, as is norepinephrine, although each acts in different responses. Once in the cleft, neurotransmitters are

active for only a short time. Enzymes in the cleft inactivate the neurotransmitters. Inactivated neurotransmitters are taken back into the axon and recycled.

Diseases that affect the function of signal transmission can have serious consequences. Parkinson's disease has a deficiency of the neurotransmitter dopamine. Progressive death of brain cells increases this deficit, causing tremors, rigidity and unstable posture. L-dopa is a chemical related to dopamine that eases some of the symptoms (by acting as a substitute neurotransmitter) but cannot reverse the progression of the disease.

2.7. Polymer Which Used in Scaffold Preparation

2.7.1. Alginate

Alginates are polyuronic acids which are major components of the cell walls of brown seaweed. Only since 1929 that alginates have been manufactured on an industrial scale. Alginates have valuable rheological properties which can be varied to a great extent by varying the degree of polymerisation of the polysaccharide or by changing the ionic environment. Over the last few years medical and pharmaceutical industries have shown increased interest in the use of biopolymers in general, and for alginates in particular (Gohel et al., 1998). The reasons for this increased interest is their usefulness in specific applications and long term safety aspects (Gohel et al., 1998). Alginates are haemocompatible and did not accumulate in any of the major organs (Rajaonarivoi et al., 1993).

2.7.1.1. Alginate structure

Alginic acid is a high molecular weight polysaccharide extracted from kelp. It is an unbranched binary copolymer of 1-4 glycosidically linked α-L-guluronic acid (G) and its C-5 epimer β-D-mannuronic acid (M) (Ottoy et al., 1997) (Figure 2.11.). The salts (and esters) of this polysaccharides are generally named alginates.

The polymer chain consists essentially of three distinct polymer segments (Ottoy, et al., 1997):

- polyguluronic acid segments (G blocks)
- polymannuronic acid segments (M blocks)

- and segments of alternating or randomly distributed mannuronic acid and guluronic acid units (MG blocks).

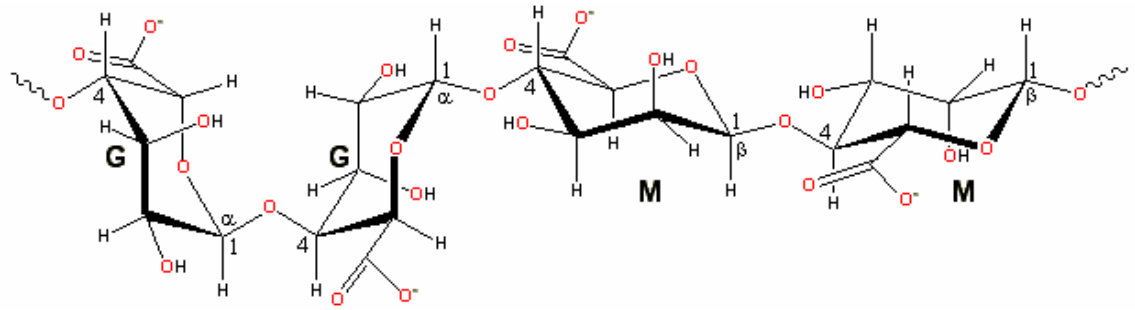

Figure 2.11. Structure of alginate.

The proportion as well as the distribution of the two monomers determines to a large extent the physiochemical properties of alginate. The proportion of the 3 polymer segments varies between each species of kelp and imparts distinctly different properties to the final product. Depending on the specific species of kelp used in manufacturing, ratios of mannuronic acid to guluronic acid content (M/G ratio), typically range from 0.4 -1.9.

Hence, alginate contains all four possible glycosidic linkages: diequatorial (MM), diaxial (GG), axial-equatorial (GM) and equatorial-axial (MG).

2.7.1.2. Sources of alginates

Alginate is the most abundant marine biopolymer and, after cellulose, the most abundant biopolymer in the world. The first scientific studies on the extraction of alginates from brown seaweed were made by the British chemist E.C. Stanford at the end of the 19th century. The major source of alginate is found in the cell walls and the intracellular spaces of brown seaweed. The alginate molecules provide the plant with both flexibility and strength, which are necessary for plant growth in the sea. Alginates are also synthesized by some bacteria (e.g. *Azotobacter* and *Pseudomonas* species). All current industrial manufacture of alginate is based on extraction of the polymer from brown algae. The M/G composition will vary from one

species of brown algae to another (Table 2.1.). Similar variations are also found in the plant during the growth season, and between different parts of the plant.

Table 2.1. Typical M/G composition and structural sequences of various species of brown algae.

SEAWEED	M/G	%M	%G	%MM	%GG
Laminaria hyperborea (stem)	0.45	30	70	18	58
Laminaria hyperborea (leaf)	1.22	55	45	36	26
Laminaria digitata	1.22	55	45	39	29
Macrocystis pyrifera	1.50	60	40	40	20
Lessonia nigrescens	1.50	60	40	43	23
Ascophyllum nodosum	1.86	65	35	56	26
Laminaria japonica	1.86	65	35	48	18
Durvillea antarctica	2.45	71	29	58	16
Durvillea potarum	3.33	77	23	69	13

2.7.1.3. Properties of alginate

For a long time scientists believed that the alginate consisted of one building block (mannuronic acid). When it turned out that the alginate consists of two building blocks (mannuronic and guluronic acid) which are found in different sequences and which give the alginates different properties for example: how and why the alginate was able to form jells, how its rate of solubility and its buoyancy can vary, etc. a new world of possibilities opened up.

Table 2.2. Properties of alginic acids, alginate salts and propylene glycol alginates.

Alginic Acids	Alginate Salts	Propylene Glycol Alginates
● Water insoluble ● Rapidly swell in the presence of water ● Solid acidulant ● White powder which contributes no odour or taste	● Hydrates readily in cold or hot water ● React with multivalent cations ● Form thermally irreversible gels ● Film formers ● Stable in pH range 4 – 10	● Hydrates readily in cold or hot water ● Reaction with calcium ions may be controlled by varying degree of esterification ● Surface active ● Reduced anionic character

2.7.1.3.1. Gel formation

The use of alginate as an immobilizing agent in most applications rests in its ability to form heat-stable strong gels which can develop and set at room temperatures. It is the alginate gel formation with calcium ions which has been of interest in most applications. However, alginate forms gels with most di- and multivalent cations. Monovalent cations (e.g. sodium, other alkali metals) and Mg^{2+} ions do not induce gelation while ions like Ba^{2+} and Sr^{2+} will produce stronger alginate gels than Ca^{2+}. The gel strength will depend upon the guluronic content and also of the average number of G-units in the G-blocks. Gelling of alginate occur when divalent cations takes part in the interchain binding between G-blocks giving rise to a three-dimensional network in the form of a gel. The binding zone between the G-blocks is often described by the so-called "egg-box model" (Gohel et al., 1998) (Fig. 2.12.).

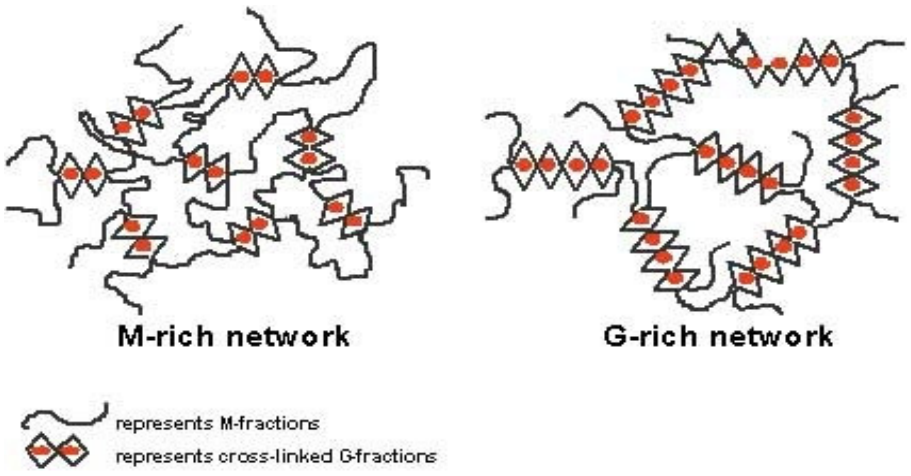

Figure 2.12. Schematic representation of the egg box model.

During gelling the concentration of divalent cations have large impact on the gel network and gel homogeneity. When the gelling takes place in presence of excess calcium, a modified egg-box model has been suggested, involving more than two alginate chains in the gelling zone. This may have an impact on the porosity of the gel. If no shrinking of the gel occurs, there may be more space in between the chains, leading to an increased porosity.

2.7.1.3.1.1. Formation of calcium alginate gel

In this study, we performed the gelation of sodium alginate with calcium. The process of gelation, simply the exchange of calcium ions for sodium ions, is carried out under relatively mild conditions. Because the method is based on the availability of guluronic acid residues, which will not vary once given a batch of the alginate, the molecular permeability does not depend on the immobilization conditions. Rather, the pore size is controlled by the choice of the starting material.

$$2\ Na(Alginate) + Ca^{++} \text{-------} > Ca(Alginate)_2 + 2\ Na^{+}$$

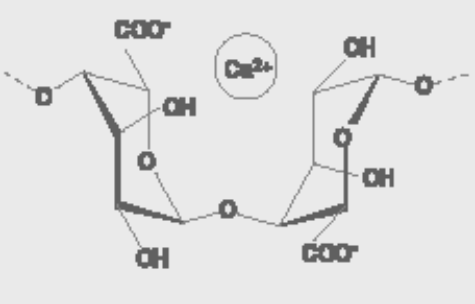

Figure 2.13. Schematic representation of the interaction of Ca^{2+} ion with alginate.

In cross-linking of alginate polysaccharide with $CaCl_2$, the calcium ion is believed to interact with five different oxygen atoms of two adjacent guluronate units in intra-chain bindings (Gohel et al., 1998) (Fig. 2.13). The ionically linked gel structure is thermostable over the range of 0-100ºC; therefore heating will not liquefy the gel. However, the gel can be easily redissolved by immersing the alginate gel in a solution containing a high concentration of sodium, potassium, or magnesium. Maintaining sodium:calcium <= 25:1 will help avoid gel destabilization.

2.7.1.3.2. Mechanical properties

Mechanical properties of alginate beads will to a large extent vary with the alginate composition. The highest mechanical strength is found when the G-content is more than about 70% and average length of G blocks (NG>1) of about 15. For molecular weights above a certain value, the mechanical strength is determined mainly by chemical composition and block structure and is therefore independent of the molecular weight (low molecular weight alginates are often preferred in biomedical

applications because they are easier to sterilize by membrane filtration). Below a certain critical molecular weight the gel forming ability is reduced. This effect will also be dependent of the alginate concentration because of polymer coil overlap.

The alginate gel as an immobilization matrix is sensitive to chelating compounds such as phosphate, lactate and citrate, presence of anti-gelling cations such as Na^{+} or Mg^{2+}. Gel strength may decrease in the following orders: $Pb^{2+} > Cu^{2+} = Ba^{2+} > Sr^{2+} > Cd^{2+} > Ca^{2+} > Zn^{2+} > Co^{2+} > Ni^{2+}$. However, in applications involving immobilization of living cells toxicity is a limiting factor in the use of most ions and only Sr^{2+}, Ba^{2+} and Ca^{2+} are considered as nontoxic for these purposes.

As alginates may form strong complexes with polycations such as chitosan (Wong et al., 2002) or polypeptides, or synthetic polymers such as polyethylenimine they may be used to stabilize the gel. When used as coating materials such complexes may also be used to reduce the porosity (Ribeiro et al., 1999; Wong et al., 2002). Alginate gels have been found stable in a range of organic solvents and are therefore, in contrast to other hydrogels, potentially useful in applications involving entrapment of enzymes in non-aqueous systems.

2.7.1.3.3. pH stability

Alginic acid is insoluble in aqueous media. However, as the pH is raised above 3, the alginic acid is partly converted to a soluble salt. Total neutralization occurs around pH 4, where the alginic acid is completely converted to its corresponding salt. Sodium, potassium, magnesium and ammonium salts are examples of water-soluble alginate salts. Neutralization by calcium, barium and other multivalent alkali materials will produce insoluble alginate salts. Sodium alginate solutions are stable in the pH range of around 4-10. Long term storage of alginate solutions outside these pH ranges is not recommended due to depolymerization of the polymer through hydrolysis. Gelation or precipitation of the alginate can occur at pH values below 4, depending on conditions. Propylene glycol alginates exhibit excellent stability in acidic solutions and are particularly effective in the pH range of 3-6.5. Alkaline conditions should be avoided because the protective effect of the ester groups will rapidly be lost through saponification.

2.7.1.3.4. Preservation

The use of a suitable preservative is recommended with all liquid or semisolid alginate formulations. Sodium benzoate, potassium sorbate and parabens are typical preservatives.

2.7.1.3.5. Storage stability

Dry alginate powders are very stable materials and do not undergo microbial spoilage. If the product is stored under cool, dry conditions in sealed containers, the only change in properties that occurs is a slow reduction in degree of polymerization. This is most easily observed as a reduction in viscosity of soluble alginates. A combination of moisture and heat may impair optimal performance of alginates, causing hydration difficulties and depolymerization, which usually results in loss of solution viscosity. Alginic acid is particularly susceptible to temperature degradation and is best stored at temperatures below 25^0C. Alginate solutions maintain good flow properties and undergo reversible viscosity decreases with increasing temperature. Depending on maximum temperature, pH and length of holding time, there may be permanent loss of some viscosity.

2.7.1.4. Applications of alginate

Alginate is currently widely used in food, pharmaceutical, textile, and paper products. The properties of alginate utilized in these products are thickening, stabilizing, gel-forming, and film-forming. Alginate polymers isolated from different alginate sources vary in properties. Different types of alginate are selected for each application on the basis of the molecular weight and the relative composition of mannuronic and guluronic acids.

General application fields of alginate; Printing and Dyeing Industry, Textile Industry, Food Industry, Medical Industry and Other Usages; Alginate can be used in paper making industry, chemical industy for daily use, casting industry, the skin of the welding electrode, the adhesion agent for fish and shrimp feed, insecticide for fruit trees, stripping mold agent of concrete, etc.

2.7.2. Chitosan

2.7.2.1. Chitin-Chitosan structure

Chitin is a non-toxic, biodegradable polymer of high molecular weight (Olabarrieta et al., 2001). After cellulose, it is the most common polysaccharide found in the nature. Chitin is structurally similar to cellulose (Upadrashta et al., 1992; Kristmundsdo´ ttir et al., 1995; Illum, 1998) (Fig. 2.14).

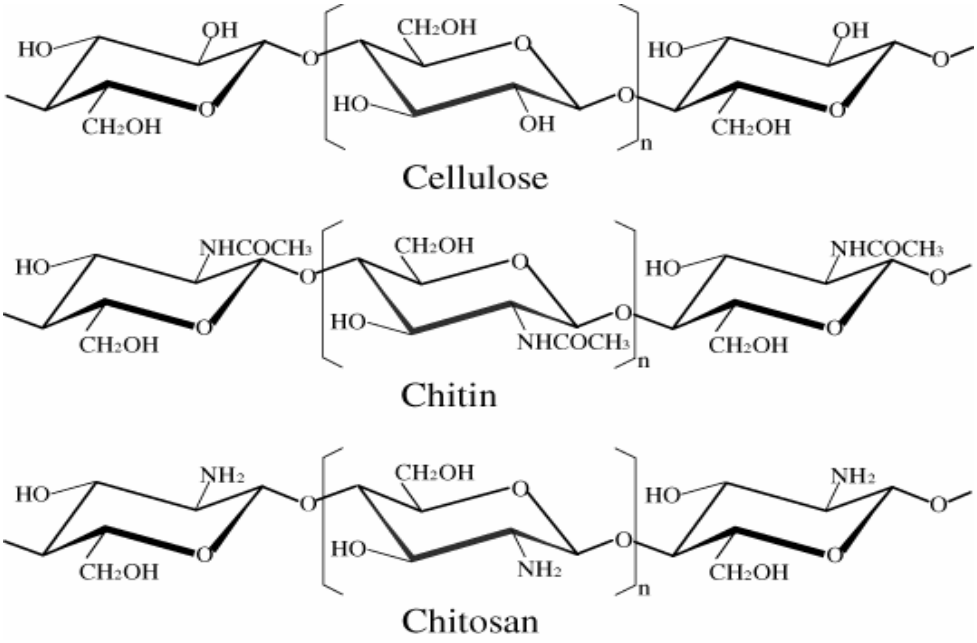

Figure 2.14. Structure of cellulose, chitin and chitosan.

Chitosan, a cationic polymer combined by β(1-4) glicosidic linkage, is the main product obtained by the alkaline deacetylation of chitin, a major structural polysaccharide found in crustaceans, insects and lower plants (Felt et al., 1998; Pauland Sharma, 2000). Chitin and chitosan have the same chemical structure. Chitin is made up of a linear chain of acethylglucosamine groups. Chitosan is obtained by removing enough acethyl groups (CH_3-CO) for the molecule to be soluble in most diluted acids. This process, called deacetylation, releases amine groups (NH) and gives the chitosan a cationic characteristic. This is especially interesting in an acid environment where the majority of polysaccharides are usually neutral or negatively charged. Chitosans are characterised by two principal factors: **viscosity and degree of deacetylation.** The control over these two parameters

allows the production of a wide range of chitosans which can be used in medical and industrial fields.

2.7.2.2. Requirements/Sources

Chitin, the second-most abundant natural polymer, is harvested mainly from the exoskeleton of marine crustaceans such as crabs, krill, lobsters and shrimp (Muzzarelli et al., 1986). It is also found in yeast and some fungi. Another inexpensive source of chitin is "squid pens," a by product of squid processing; these are small, plastic-like, inedible pieces of squid that are removed prior to eating. In the creatures where chitin is found, it is in different percentages depending on the place. As you can see from the chart of all the creatures (Table 2.3.), crabs contain the largest percentage of chitin. (Muzzarelli: All numbers are approximate).

Table 2.3. Percentage of chitin in creatures.

Fungi	5-20%
Worms	20-38%
Squids/Octopus	3-20%
Scorpions	30%
Spiders	38%
Cockroaches	35%
Water Beetle	37%
Silk Worm	44%
Hermit Crab	69%
Edible Crab	70%

2.7.2.3. Properties of chitosan

Chitosan is a polysaccharide derived from chitin which exhibits numerous interesting physicochemical and biological properties (Domard et al., 1998).

2.7.2.3.1. Chitosan's chemical properties

The potentiality of chitosan in sustained release systems has been assigned to its polymeric character including its gel and film forming properties. It has to be mentioned that chitosan demonstrates slow release properties due to its swelling nature in acid medium; on the other hand, it has been found to act as a disintegrant when in medium pH 6.8 or higher. Attempts have been made to diminish the medium dependent disintegrant activity of chitosan.

Table 2.4. Chemical properties of chitosan

Linear polyamine (poly-D-gulconsamine)
Reactive amino groups
Reactive hydroxyl groups available
Chelates many transitional metal ions

2.7.2.3.2. Chitosan's biological properties

Chitosan is a natural polysaccharide (N-deacetylated-2-acetamido-2-deoxy-β-D-glucan). It is a biodegradable, biocompatible positively-charged polymer, which shows many interesting properties (Muzzarelli et al., 1988; Patel and Amiji, 1996). Moreover, chitosan is a virtually non-toxic polymer with a wide safety margin and it can be used in drug delivery systems as a novel carrier for both oral and intravenous administration (Hirano et al., 1988; Jameela et al., 1996).

Table 2.5. Biological properties of chitosan

- Biocompatible
  - -natural polymer
  - -biodegradable to normal body constituents
  - -safe, non-toxic
- Binds to mammalian and microbial cells aggressively

- Regenerative effect on connective gum tissue
- Accelerates the formation of osteoblasts reponsible for bone formation
- Hemostatic
- Fungistatic
- Spermicidal
- Antitumor
- Anticholesteremic
- Accelerates bone formation
- Central nervous system depressant
- Immunoadjuvant

2.7.2.3.3. Chitosan's cationic properties

Chitosan is polycationic at pH 6 and interacts readily with negatively charged substances such as proteins, anionic polysaccharides (alginate, carrgeenan), fatty acids, bile acids and phospholipids due to the high density of amino groups present in the polymer (Knorr, 1984; Muzzarelli, 1996). Perhaps less predictably, chitosan also selectively chelates metal ions such as iron, copper, cadmium and magnesium. The amino group of the 2-amino-2deoxy-D-glucose-(glucosamine) unit plays an important role as a chelating agent.

Table 2.6. Cationic properties of chitosan

- Linear polyelectrolyte
- High charge density
- Excellent flocculent
- Adheres to negatively charged surfaces
- Substantive to hair, skin
- Chelates metal ions
  Iron (Fe), Cupper (Cu)
  Toxic metals (Cd, Hg, Pb, Cr, Ni) and Radionucleides (Pu, U).

2.7.2.3.4. Chitosan's solution properties

Table 2.7. Solution properties of chitosan .

Free amine (NH_2)

- Soluble in acidic solutions
- Insoluble at pH's > 6,5
- Insoluble in H_2SO_4
- Limited solubility in H_3PO_4
- Insoluble in most organic solvents

Cationic amine (NH_3^+)

- Soluble at pH's < 6,5
- Forms viscous solutions
- Solutions shear thinning
- Forms gels with polyanions
- Will remain soluble in some alcohol-water mixtures

2.7.2.4. Application of chitosan

Chitosan has found numerous applications in various fields (Hirano, 1996) such as waste-water treatment (Dean et al., 1992), agriculture (Hadwiger, 1989), cosmetics (Lang et al., 1989) and food processing (Roller et al., 1999). Due to its biocompatibility, biodegradability and bioactivity, it is more and more considered as a very interesting substance for diverse applications as a biomaterial (Chandy et al., 1990).

General application fields of chitosan; Cosmetic, Medicine, Dietetics, Water Treatment and Pollution Control, Agriculture, Paper Manufacture, Photography, Food.

2.8. Cellular Application İn Nerve Guide Systems

No satisfactory method currently exists for bridging neural defects. Autografts lead to inadequate functional recovery, and most available artificial neural conduits possess unfavorable swelling and pro-inflammatory characteristics. There are a lot of nerve guide samples in literature: Poly(1,3-trimethylene carbonate) (poly(TMC)) scaffold (Pˆego et al., 2003), NGF-containing poly(phosphoester) (PPE) microspheres were loaded into silicone or PPE conduits (Xu et al., 2003), agarose scaffold with uniaxial linear pores was developed for using freeze-dry processing (Stokols et al., 2004), two polyphosphoesters (PPEs), P(BHET-EOP/TC) and P(DAPG-EOP), as well as poly(lactide/glycolic acid) (PLGA), were used to fabricate microspheres by a W/O/W emulsion and solvent evaporation/extraction method (Xu et al., 2002), hyaluronan-based conduit for peripheral nerve repair (Jansen et al., 2004), genipin-cross-linked gelatin peripheral nerve guide conduit material (Chen et al., 2005). In this study, we examined the biocompatibility of a novel biodegradable chitosan coated alginate scaffold, for neural reconstruction applications, as the material possesses favorable mechanical property and degradation characteristics.

3. EXPERIMENTAL

3.1. Materials

Alginic acid sodium salt from brown algae and chitosan (MMW) were purchased from Fluka. Hexamethyldisilane (HMDS), sodium hydroxide (NaOH), Na_2HPO_4, acetic acid, $CaCl_2.2H_2O$ (as a crossslinker), ethanol, isopropanol, hydrochloric acid and D(+)-Glucose monohydrate were purchased from Merck. 3,5-Dinitrosolycylic Acid ($C_7H_4N_2O_7$) was purchased from Sigma. Sodium sulfide was purchased from Canalar. Sodium potassium tartarate was purchased from Panreac. Phenol was purchased from Carlo Erba. KH_2PO_4 was purchased from Acros Organic. Glutaraldehyde (25%) and MTT ($C_{18}H_{16}BrN_5S$) were purchased from Serva. May-Grunwalds Eosine-Methylen blue and Giemsa's azur Eosin-Methylene blue solution were purchased from Merch (Germany).

L-929 cell lines used in cell culture studies were obtained from the tissue culture collection of Foot-and-Mouth Disease Institute of Ministry of Agriculture & Rural Affairs of Turkey. All the chemicals used in cell culture studies were purchased from Biological Industries (Israel). These chemicalls are; L-Glutamine solution (200 mM), antibiotics (Pen-Strep solution (penicilin: 10.000 units/mL, streptomicyn: 10 mg/mL)), Trypsin-EDTA solution (with fenol red, 0.05% trypsin& EDTA (1:5000)), fetal bovine serum (FBS), cell culture media (RPMI 1640 with HEPES (25 mM)). Cell culture flasks and other plastic material were purchased from Corning (USA).

3.2. Preparation of Scaffold

Freeze/dry processing is an alternative method for producing porous scaffolds that does not require additional chemicals, relying instead on the water already present in hydrogels to form ice crystals that can be sublimated from the polymer, creating a particular micro-architecture (Stokols et al, 2004). The direction of growth and size of the ice crystals are a function of the temperature gradient, linear, radial, and/or random pore directions and sizes can be produced with this method (Madihally et al., 1999). Two different procedures were used on freeze-dry method to create the alginate scaffolds. Sodium alginate salt was dissolved in water (3%-9%, w/v) by using sonicator and sodium alginate gel was injected into glass tube of 5mm diameter and

7cm length. The tube was centrifuged to remove air bubbles into the alginate gel. First procedure, alginate scaffolds were prepared by directly immersion of the glass tube which contains alginate gel into the liquid nitrogen (random freezing). In the second procedure, we prepared the alginate scaffolds with oriented freezing. The glass tube containing alginate gel was placed in an insulating styrofoam container. The seperation funel was placed onto the glass tube which in styrofoam, then liquid nitrogen was pour onto the alginate gel. The freezing time for two different procedure was 45 min., after interaction of sodium alginate gel with liquid nitrogen, the samples were put into the freezer at -80^{0}C overnight, after that were lyophilized overnight. Scaffolds were removed from the tubes, and crosslinked with $CaCl_2.2H_2O$ (5-20%, w/v) and MMW-chitosan (0.25-1%, w/v), respectively.

Table 3.1. Formulation used for the preparation of different alginate scaffolds.

Sodium Alg. Concentration (%, w/v)	$CaCl_2.2H_2O$ Concentration (%, w/v)	Chitosan Concentration (%, w/v)
Effects of Sodium Alginate Concentration		
3	20	1
6	20	1
9	20	1
Effects of $CaCl_2.2H_2O$ Concentration		
3	5	1
3	10	1
3	20	1
Effects of the Chitosan Concentration		
3	20	1
3	20	0.50
3	20	0.25

3.3. Characterization of Scaffold

3.3.1. Morphological evaluation

Alginate scaffolds which were prepared using different freezing procedure and characterized by scanning electron microscope (SEM) and light microscope. For SEM, sectioned scaffolds were attached to sample stubs, the samples were coated with 5-10 Å thick gold, and the SEM micrographs were obtained. In the light microscope studies; sectioned scaffolds were placed to coverslips and the optic micrographs were taken.

3.3.1.1. Microstructure analysis

Microstructure analysis of alginate scaffolds was performed using the optic micrographs. Proximal and distal surfaces of scaffolds images were taken. The pore size of the scaffolds was measured using Image-Pro Express software (Media Cybernetics, USA).

3.3.2. FTIR studies

FTIR spectras were taken for sodium alginate, calcium alginate and chitosan coated calcium alginate scaffolds. FTIR spectras were obtained using FTIR spectrophotometer (FTIR, Schimadzu, Japan). In a typical procedure 0.1 g of sample was completely mixed with IR grade KBr (Merk, Germany) and pressed (with 10 tons) into the tablet and the spectrum was recorded.

3.3.3. Water uptake

Water uptake capacity of chitosan coated calcium alginate scaffolds was determined using gravimetric method. The weight of dry scaffolds which have 5mm diameter and 7mm length were measured and placed into the silk filter (100-120 hole in cm^2) which in the shape of bundle, then scaffolds with silk filter were immersed into phosphate buffered saline (PBS) solution (pH 7.4) at 37^0C. And weight of swollen samples periodically were recorded to determine water uptake capacity of the

scaffolds. The sample weight was determined by first blotting the sample with filter paper to remove absorbed water on the surface and weighted immediately on electronic balance (Metler, Switzerland).

The percentage of water uptake of chitosan coated calcium alginate scaffolds was calculated from the following equation;

$$S = \frac{w_t - w_0}{w_o} \times 100$$

where S is the percentage of water uptake(%), w_t denotes the weight of the scaffold at time t and w_0 is the initial weight of the scaffold. The effects of alginate, crosslinker and chitosan concentration on the water uptake capacity were investigated to characterize the chitosan coated calcium alginate scaffold.

3.3.4. Hydrolysis/Degradation

Mass degradation of hydrated chitosan coated calcium alginate scaffolds was measured for 3-months period. Twelve dry scaffolds of 5mm diameter and 7mm length were weighted and then immersed in PBS (pH=7.4) containing 0.02 wt/vol% of NaN_3 (Sigma, USA) at 37^0C. NaN_3 was added to PBS solution to prevent bacterial growth. PBS solution was replaced with fresh solution every week and pH change was recorded for every week. Each scaffold was removed from the water bath every 7 days, lightly blotted on filter paper until all adsorbed water was removed, dried into desicator, and then reweighted. Mass loss of the scaffolds was defined as:

mass loss (wt%) = $100X(w_i\text{-}w_r)/w_i$, where w_i represents the initial dry sample weight and w_r represents the remaining weight of the sample after drying.

3.3.5. Permeability studies

The permeability of chitosan coated calcium alginate scaffolds to molecules ranging from the size of glucose (MW=180) to HSA (MW=66,000) was tested at 37^0C. Chitosan coated calcium alginate scaffolds of 5mm diameter and 7mm length were

each filled with glucose and HSA. Then these samples were placed to PBS (pH=7.4) at 37^0C. The amount of glucose and HSA released was determined with UV spectroscopy at 540 nm and 280 nm, respectively. Glucose estimation test was used to determine the released amount of glucose in PBS (Miller, 1959). The diffusion rates of materials across the scaffolds were analysed for 1 month.

3.3.6. Mechanical testing

Elastic properties and shear modulus of dry and wet scaffolds were determined by using a Zwick Z010 model Universal Testing Instrument and uniaxial extension (load cell 1 kN) module. The crosshead speed was 5 mm/min.

3.3.7. Biocompatibility Tests

3.3.7.1. *In vitro* haemocompatibility tests

In this part of the study, chitosan coated calcium alginate scaffolds were exposed to some coagulation tests to investigate whether they affect the coagulation cascade or not. Coagulation tests contain activated partial thromboplastin time (APTT), thrombin time (TT), fibrinogen time and protrombin time (PT). The clotting characteristics of the plasma were taken as the blank and the scaffolds were compared with the blank.

3.3.7.1.1. *In vitro* haemocompatibility test procedure

The citrated whole blood taken from a healthy donor was centrifuged at 4000 rpm for 7 min. at room temperature to obtain platelet poor plasma (PPP). The samples placed in a polystyrene 24-well plate dish were in contact with 1ml of PPP for 30 min. at 37^0C (Yoshioka, et al., 2003). All analyzes were triplicated. The plasma samples were tested with the following procedure:

- The clotting balls were put in each test tubes.
- The automatic pipette was filled with test reagent, Neoplastine for PT, $CaCl_2$ for APTT and Fibri Prest for Fibrinogen.

- Plasma samples were added to clotting ball containing test cuvettes (50 µl plasma for PT, 50 µl plasma and 50 µl APTT reagent for APTT, and 1/20 diluted 100 µl plasma for fibrinogen test).

- The samples were incubated for definite time (50 seconds for PT and fibrinogen and 170 seconds for APTT) at 37^0C.

- After incubation, cuvettes which contains the samples were transferred immediately to testing part of the analyzer and the specific test reagents were added (100 µl for PT and 50 µl for APTT and fibrinogen).

- The results were taken after the measuring time.

3.3.7.1.2. ***In vitro*** **haemocompatibility test device**

In vitro haemocompatibility tests of chitosan coated calcium alginate scaffolds were done with STA 4 Compact Blood Coagulation Analyzer, (Diagnostica Stago, France) using the required test kits such as PTT, APTT, TT, Fibrinogen and D–Dimer. (Diagnostica Stago, France).

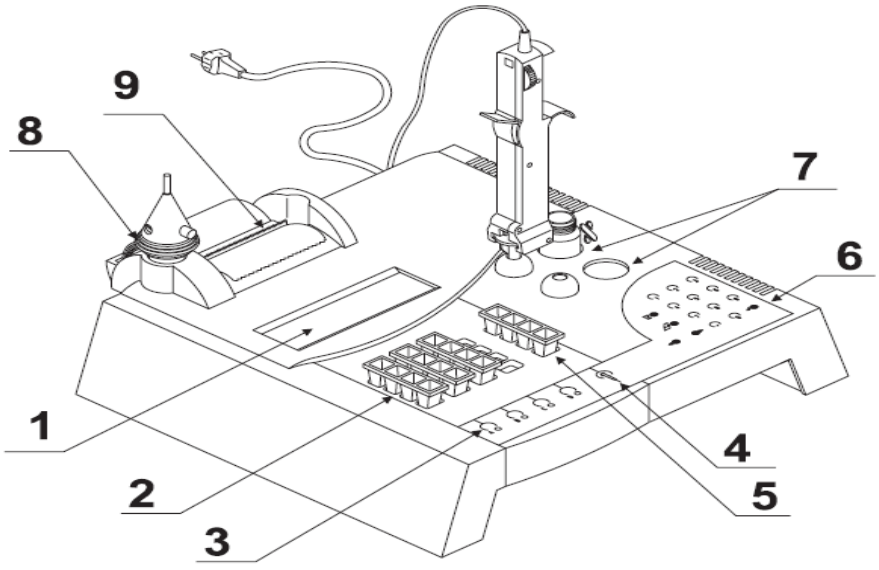

Figure 3.1. Blood coagulation test device.

1 - Back light liquid crystal display

2 - Incubation area (4 columns of 4 cells) thermostated at 37^0C

3 - Control keys for incubation timers A to D

4 - Control key for pipette

5 - Measurement area thermostated at 37^0C

6 - Numerical keyboard, see following description

7 - Two 37^0C thermostated reagent and multipette storage positions

8 - Single storage position for the ball dispenser

9 - Thermal printer

3.3.7.1.3. Principle of clot determination

Clot determination principle consists of measuring the variations of the ball oscillation amplitude through inductive sensors.

The ball has a pendular movement obtained

- thanks to the two curvated rail tracks of the cuvettes
- and an alternate electro-magnetic field created by two independent coils

The oscillation amplitude is constant when the environment has a constant viscosity. The oscillation amplitude decreases when the environment viscosity increases.

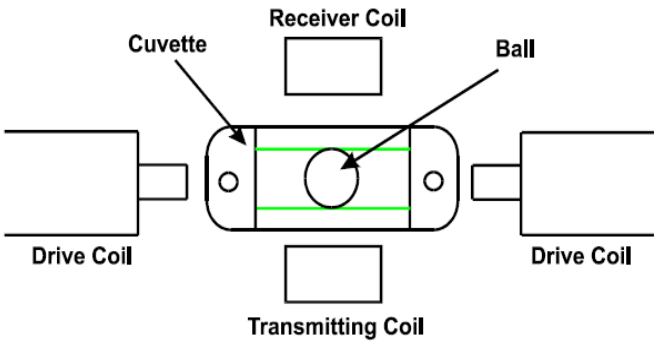

Figure 3.2. Clot sensing system.

Constant pendular swing of the ball at constant medium viscosity is achieved on through application of an electro-magnetic field created alternately at opposite sides of each measurement well . The intensity of magnetic field can be varied depending on the tests to be carried out (PT, APTT...) and on the expected clot. The detection system of the oscillation amplitude variations is based on two measurement coils. The transmitting coil emits an electro-magnetic field. The signal received by the receiver coil depends on the ball position in the cuvette. An algorithm uses these oscillation amplitude variations to determine the clotting time.

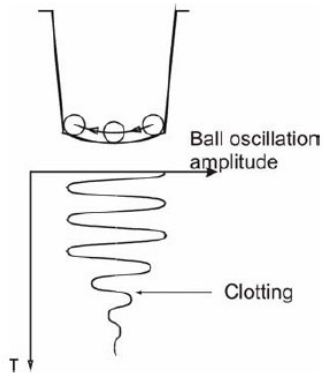

Figure 3.3. Clot forming.

3.3.7.2. Cell attachment study

In vitro biocompatibility was tested by co-incubation of chitosan coated calcium alginate scaffolds with mouse connective tissue fibroblast cells (L-929 cell line, Foot-and-Mouth Disease Institute (Ankara) of Ministry of Agriculture & Rural Affairs of Turkey) for 2 days. 24-well plate was used for cell attachment study. Firstly, surface of the 24-well plate was coated with parafilm to block the cell attachment onto the well. Then scaffolds were placed to the 24-well plate and plate and scaffolds were sterilized in laminar flow cabin under UV radiation for 30 minutes. After that growth media consist of 90% RPMI 1640 with L-Glutamine + 10% FBS (Bio-Industries, USA) was poured onto the scaffolds to improve the cell attachment and waited for overnight in incubator (Revco, USA) supplied with 5% CO_2 at 37^0C. Precultured L-929 cells were added into the well and incubated in incubator for 2 days. After 2 days, firstly, cells were dyed with May-Grunwalds and Giemsa's azur to see that the

cells attached to the scaffolds or not. We observed the cell attachment to the scaffold by optic microscope and then, the cells were fixed to the scaffolds with 3% glutaraldehyde for 30 minutes and dehydrated in a series of graded ethanols (30%, 35%, 50%, 70%, 85%, 95% and 100%) for 5 minutes each. Then samples were keep into the HMDS solution for 5-15 minutes and after this, the samples were dried at room temperature for 30 min, then put into the desicator for 24 hours. Samples were then kept in refrigerator for SEM visualization.

3.3.7.3. MTT assay

MTT [3-(4,5-dimethylthiazol-2-yl)-2,5-diphenyltetrazolium bromide] assay, first described by Mosmann in 1983, is based on the ability of a mitochondrial dehydrogenase enzyme from viable cells to cleave the tetrazolium rings of the pale yellow MTT and form a dark blue formazan crystals which is largely impermeable to cell membranes, thus resulting in its accumulation within healthy cells. Dead cells don't produce formazan crystals. The proliferative activity of cultured cells with chitosan coated calcium alginate scaffolds was determined with the MTT colorimetric assay. All the samples in 96 well plate were sterilized for 30 min. under UV radiation and then culture medium was added into the wells. L-929 mouse fibroblasts were seeded in each well of 96 plate at a concentration of 1×10^4 cells/well. The incubation was performed under CO_2 (5%) atmosphere at 37^0C for different incubation times (24 h., 48 h., 72 h., 96 h.). After each incubation time, scaffolds were removed from the respective wells. Only the cells adhered to the well walls were incubated with a tetrazolium salt solution (MTT, 5mg/ml in RPMI without phenol-red) for 4 h., in incubator at 37^0C. During this time, yellow MTT solution is transformed by the cells mitochondrial dehydrogenase into insoluble blue formazan. By measuring the amount of formazan produced it is possible to measure mitochondrial activity, and, as a consequence, cell viability. At the end of the incubation period, the MTT solution was removed and then 100 µl/well isopropanol/HCl (0.4 N) solution was added to each well in order to dissolve formazan crystals. The 96 well-plate was mixed at 37^0C, until the purple color was uniform. After complete solubilization of the dark-blue crystal of MTT formazan, the absorbance of the content of each well was read in ELISA reader at 570 nm. The cell viability was calculated by the normalization of optical density (OD) to the negative control.

4. RESULTS AND DISCUSSION

4.1. Preparation and Characterization of Scaffold

The chitosan coated calcium alginate scaffolds were prepared by freeze-dry technique as described before. Morphological investigation, functional groups analysis, microstructure analysis, water absorbability, hydrolysis/degradation profile, mechanical strength, permeability and biocompatibility studies were performed to characterized the chitosan coated calcium alginate scaffolds

4.1.1. Morphological evaluations

Morphological evaluation of the chitosan coated calcium alginate scaffolds was made by using light microscope and scanning electron microscope (SEM) images.

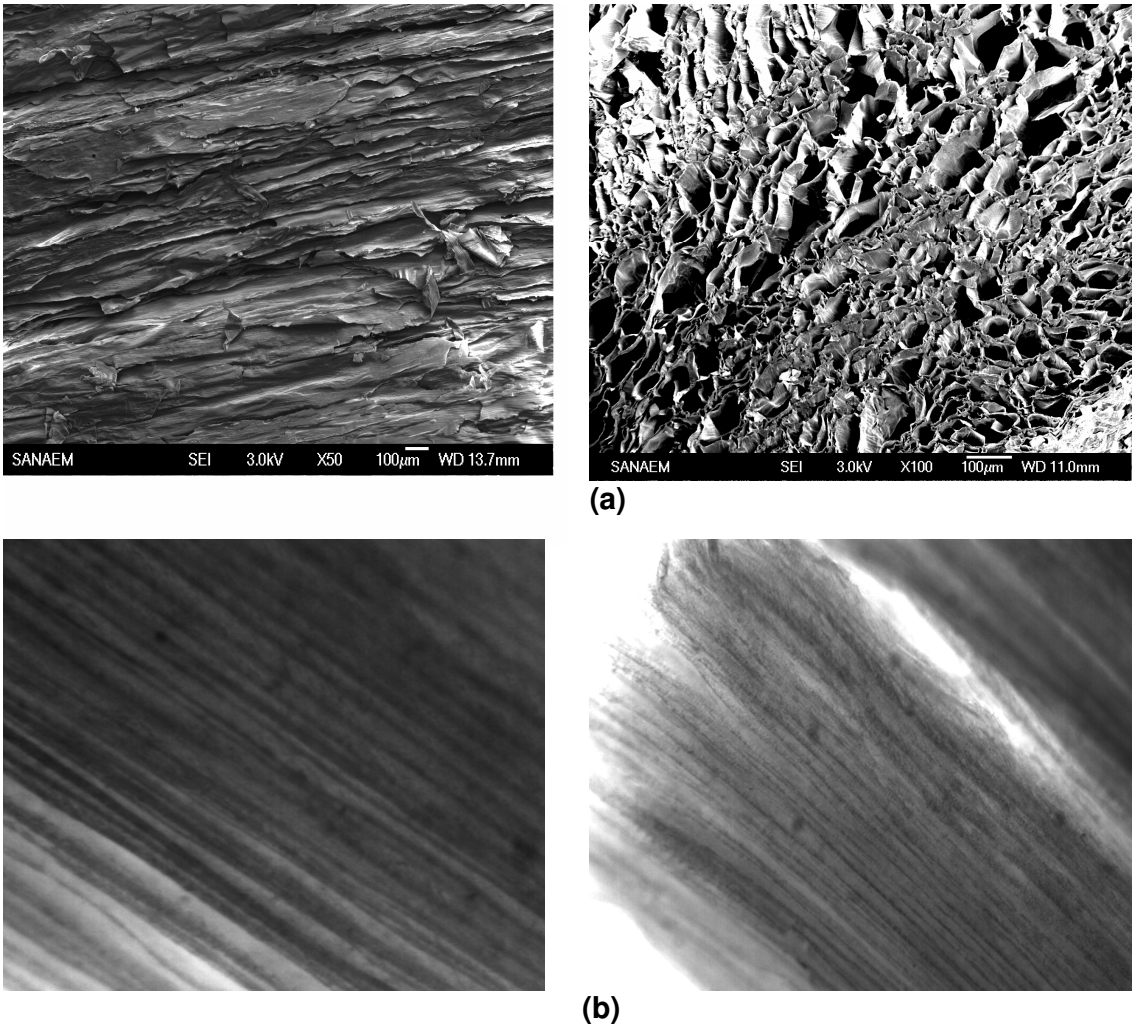

Figure 4. 1. (a) SEM and (b) Light microscope, micrographs of scaffolds.

As seen in SEM and light microscope images (Figure 4.1), the linear uniaxial freezing gradient produced final scaffolds with linear pores in a honeycomb arrangement. Pores extended linearly through the full extent of scaffolds, evidenced by coloured solution movement. One end of the scaffolds was immersed to the coloured fluid, and fluid was discharged only from the opposite end of the scaffold and did not immerse from the side walls.

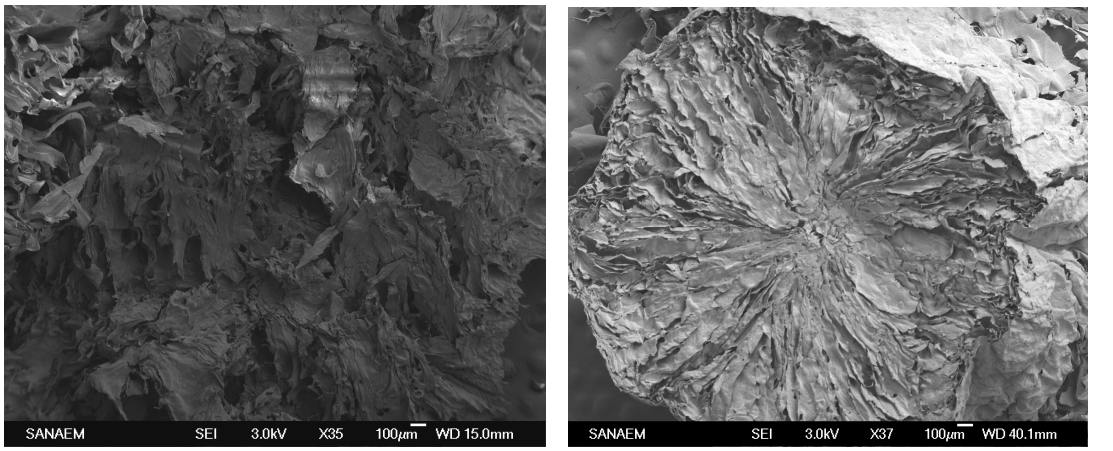

(a)

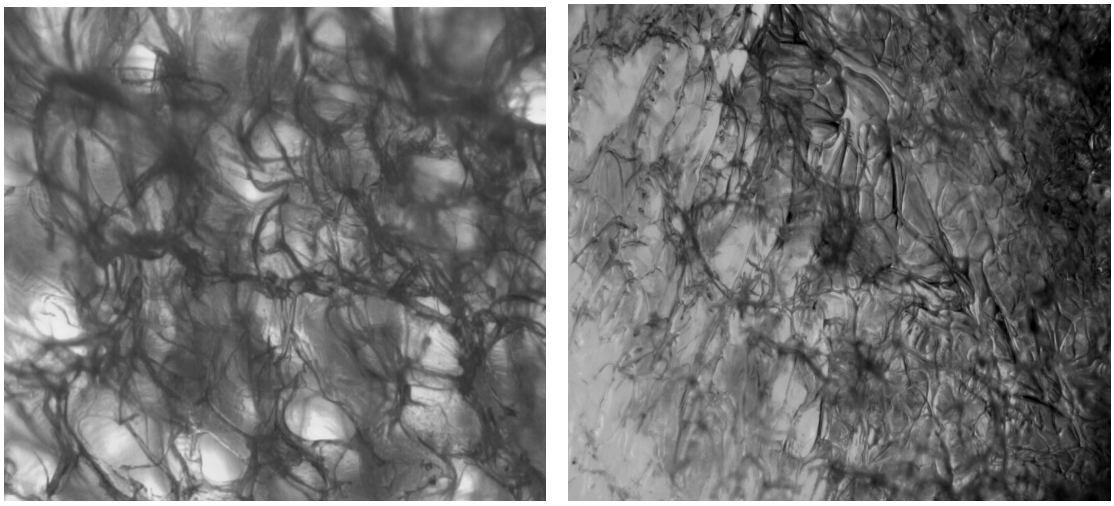

(b)

Figure 4.2. Images of scaffolds which prepared by direct immersion technique by (a) SEM and (b) Light microscope.

As seen in SEM and light images (Figure 4.2), the scaffolds which directly immersed to the liquid N_2 or in other words have random freezing gradient have porous structure. Direction of the pores are outer of the scaffold to the central of the scaffold. It has random pores not linear pores. As a result, the direction of growth and size of

the ice crystals are a function of the temperature gradient, linear, radial, and/or random pore directions and sizes can be produced with freeze-dry methodology (Madihally et al., 1999).

4.1.1.1. Microstructure analysis

Theoretically, scaffolds created for guiding axonal regeneration should have pores small enough to physically align and restrict the direction of growing axons, yet large enough to allow for vascularization and the infiltration of cells which might support regeneration (Stokols et al., 2004). To meet these requirements, we targeted production of a hypothetically ideal pore size nearly 100 μm. Most effective parameter on the pore size of scaffold is sodium alginate concentration. The pore size-size distribution of the chitosan coated alginate scaffolds was determined by using Image-Pro Express (MediaCybernetics, USA).

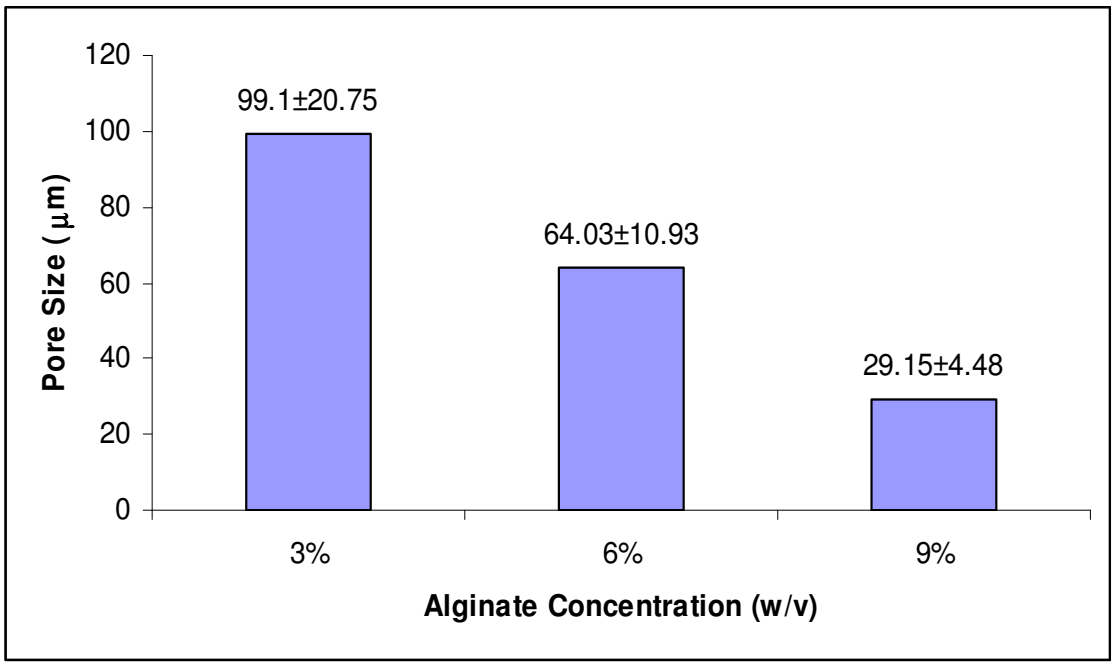

Figure 4.3. The effects of sodium alginate concentration on the pore size of the scaffold (3%, 6%, 9% w/v).

We investigated the effects of sodium alginate concentration on scaffolds' pore size by changing concentration as 3%, 6% and 9% (w/v). The other parameters which are 20% $CaCl_2.2H_2O$, 1% chitosan concentration were fixed during the preparation of the

scaffold. Pore size decreased with increasing of sodium alginate concentration because of viscosity of the gel increased. The observed results were given in Figure 4.3.

4.1.2. FTIR studies

The alginate scaffolds, calcium alginate scaffolds, chitosan and chitosan coated calcium alginate scaffolds were characterized by using FTIR spectra. Changes in the absorption bands were investigated in the 500–4000 cm^{-1} region. The FTIR spectra of sodium alginate scaffold, calcium alginate scaffold, chitosan and chitosan coated calcium alginate scaffold are shown in Figure 4.5. The characteristic peaks of sodium alginate scaffold are 3422 cm^{-1} (O-H) band, 1617 cm^{-1} (COO) band and 1094 cm^{-1}, 1030 cm^{-1} (C-O-C) bands (Figure 4.5.a). The characteristic bands of calcium alginate scaffold are 3428 cm^{-1} (O-H) band, 1631 cm^{-1} (COO) band and 1081 cm^{-1}, 1026 cm^{-1} (C-O-C) bands (Figure 4.5.b). Replacement of Na^{+} ions with Ca^{2+} ions in alginate, the intensity of (O-H), (COO) and (C-O-C) bands decrease because Ca^{2+} ions interact with 5 different oxygen ions in alginate structure (Figure 4.4).

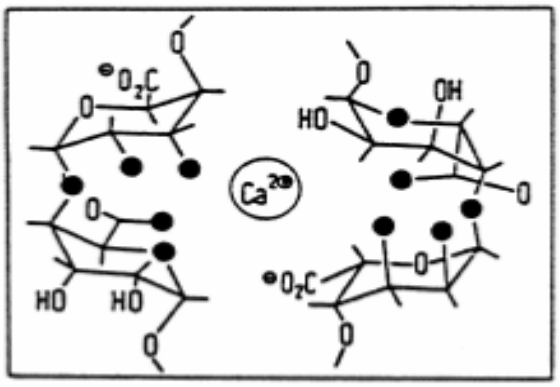

Figure 4.4. Interaction of Ca^{2+} ions in alginic acid.

The spectrum of chitosan (Brugnerotto et al., 2001) (MW of chitosan: MMW) shows the characteristic absorption bands at 3434 cm^{-1} (O-H), 1644 cm^{-1} (Amine I) and 1157 cm^{-1} (anti-symmetric stretching of the C–O–C bridge), 1102 cm^{-1} and 1028 cm^{-1} skeletal vibration involving the C–O stretching (Fig. 4.5.c).

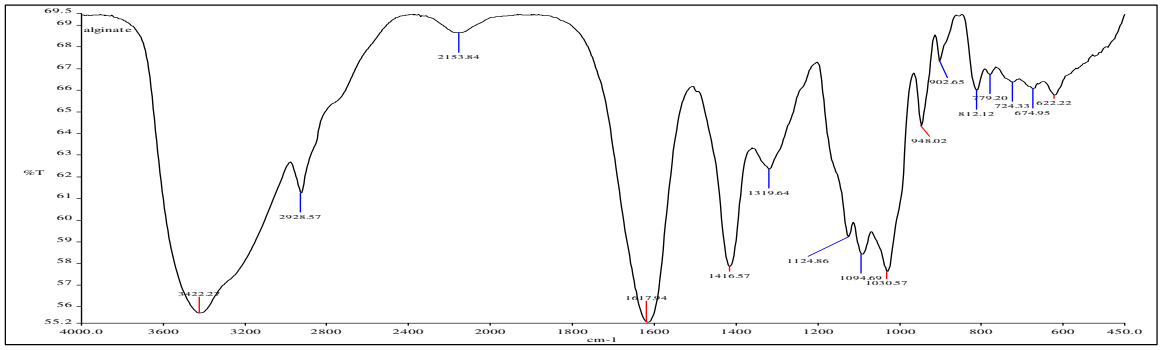

(a)

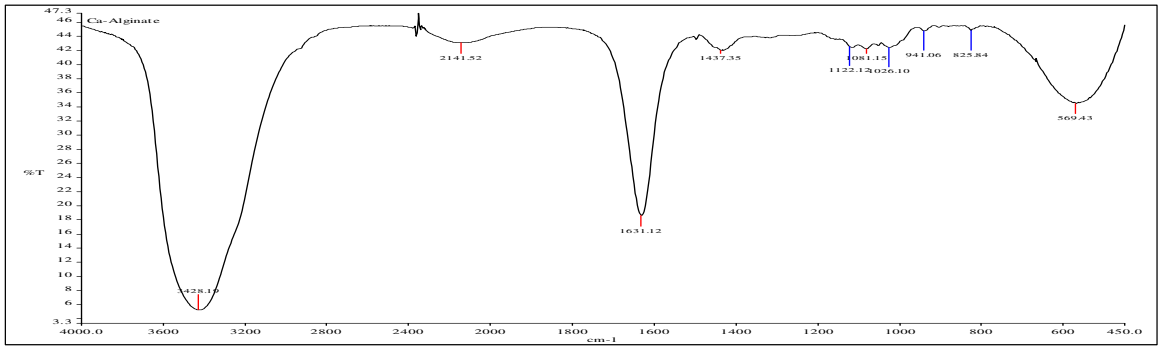

(b)

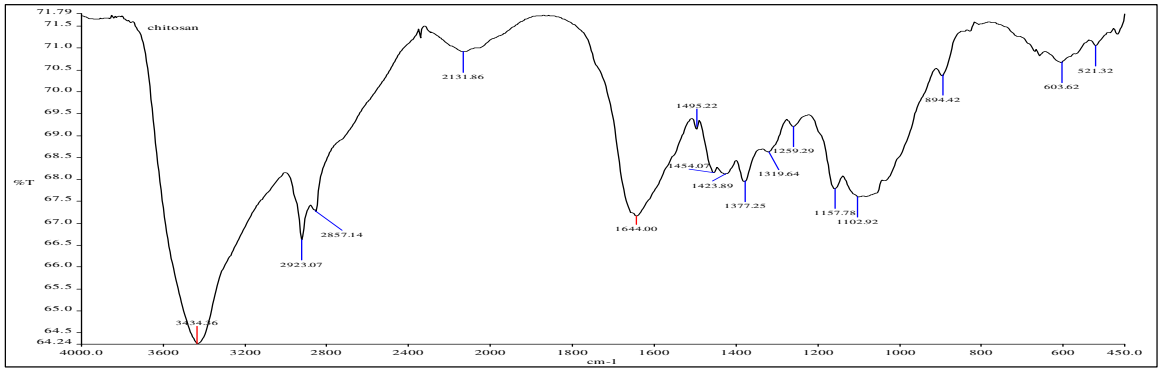

(c)

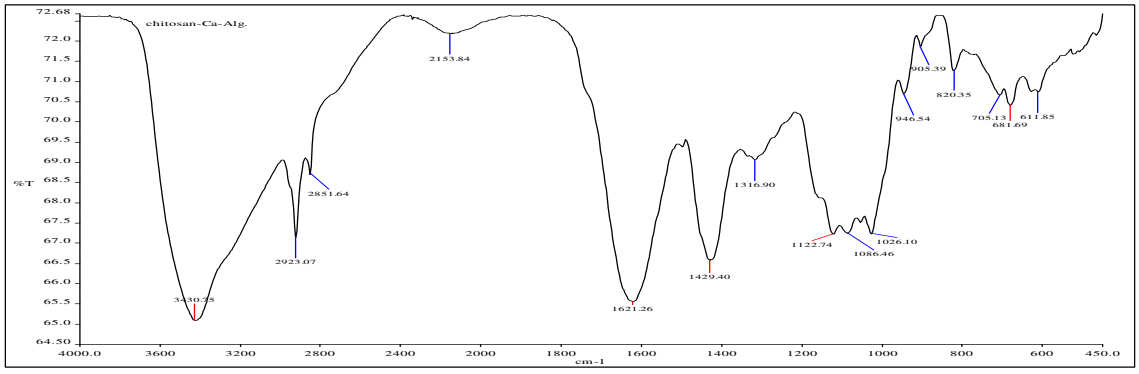

(d)

Figure 4.5. FTIR spectrum of (a) sodium alginate (b) calcium alginate scaffold (c) chitosan (MMW) (d) Chitosan coated calcium alginate scaffold (MMW chitosan).

Polyionic complex formation involved between alginate and chitosan with ionic interaction between the negatively charged carboxyl group of alginate and the positively charged ammonium group of chitosan (Fig. 4.6.). After polyionic complex formation, intensity of O-H band of calcium alginate at 3428 cm^{-1} increased and N-H band of chitosan at 1644 cm^{-1} and (COO) band of calcium alginate at 1631 cm^{-1} overlaped.

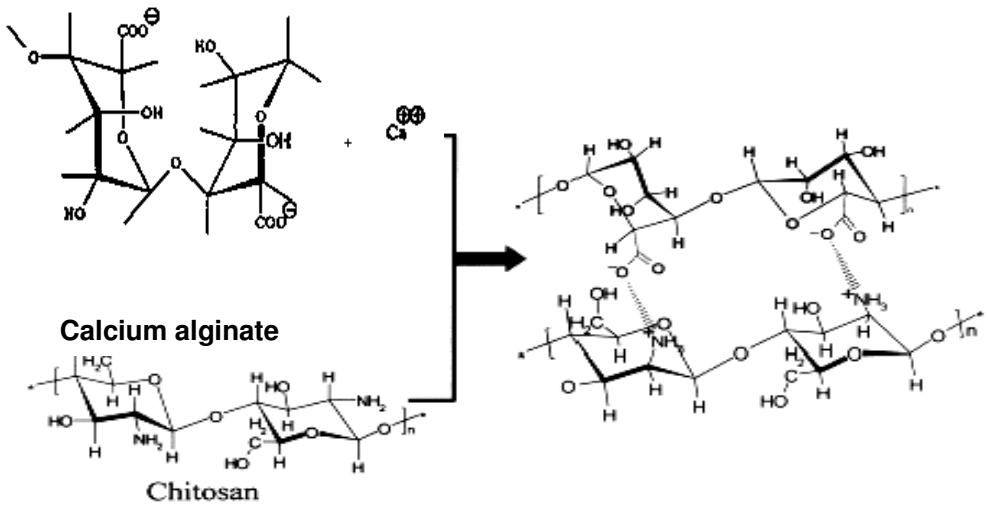

Figure 4.6. Schematic representation for the ion complex formation reaction between the anion group ($–COO^-$) of calcium alginate and the protonated cation group ($–NH_3^+$) of chitosan.

4.1.3. Water uptake

Water uptake studies were performed by using silk filter which represented in Figure 4.7.

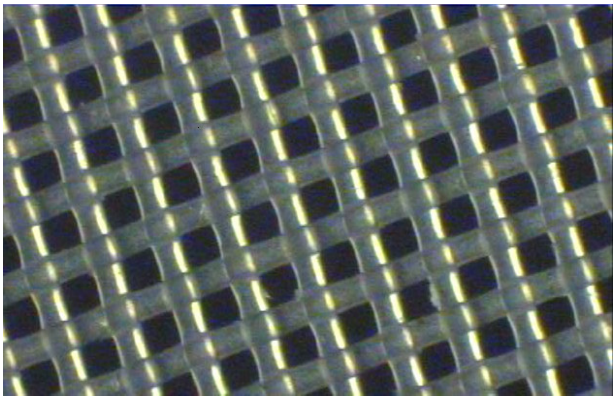

Figure 4.7. Structure of the silk filter.

The most effective parameters on the water uptake capacity of chitosan coated calcium alginate scaffolds were selected as alginate concentration, $CaCl_2.2H_2O$ concentration and chitosan concentration. These effects were discussed individually in the following subsections.

4.1.3.1. Effects of sodium alginate concentration on water uptake

The sodium alginate concentration was an effective parameter on the water uptake capacity of chitosan coated calcium alginate scaffolds in PBS at 37^0C. To investigate the effects of sodium alginate concentration on water uptake behavior of scaffolds, three different sodium alginate concentration were examined as 3%, 6% and 9% (w/v). While alginate concentrations were changed, other parameters were fixed as 20%(w/v) $CaCl_2.2H_2O$, 1%(w/v) chitosan. The relationship between alginate concentration and water uptake capacity of scaffolds was shown in Figure 4.8.

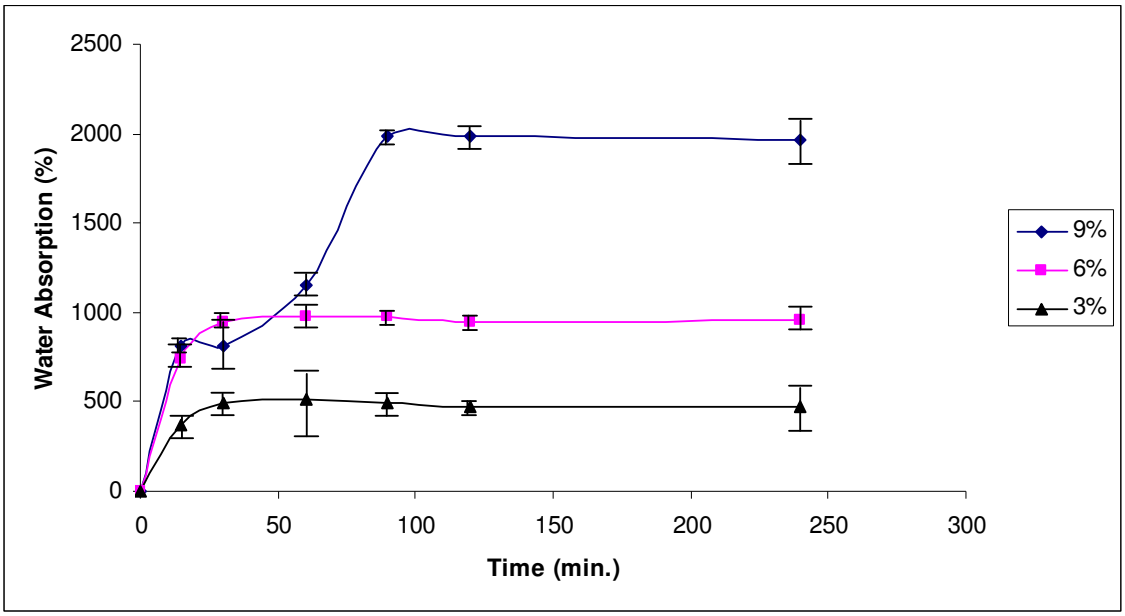

Figure 4.8. The effects of sodium alginate concentration (9%, 6%, 3%) on water uptake capacity of chitosan coated calcium alginate scaffolds.

Water uptake capacity changed approximately between 500% and 2000% depending on sodium alginate concentration. Maximum water uptake ratio (i.e. around 2000%) was obtained at high sodium alginate concentration (9%, w/v), because while sodium alginate concentration increased, crosslinker concentration was constant, so that

crosslinker density decreased and water easily diffused to the scaffold. As a result; water absorption capacity increased with increasing of sodium alginate concentration.

4.1.3.2. Effects of $CaCl_2.2H_2O$ concentration on water uptake

$CaCl_2.2H_2O$ concentration was an effective parameter to determine the water absorption capacity of chitosan coated calcium alginate scaffolds in PBS at 37^0C. $CaCl_2.2H_2O$ concentration was changed as 5%, 10% and 20%(w/v), other parameters were fixed as 3%(w/v) alginate concentration, 1%(w/v) chitosan concentration while scaffolds were prepared. $CaCl_2.2H_2O$ concentration directly affected the tightness of the scaffold. When $CaCl_2.2H_2O$ concentration increased, water absorption capacity of scaffold decreased. These results were given in Figure 4.9.

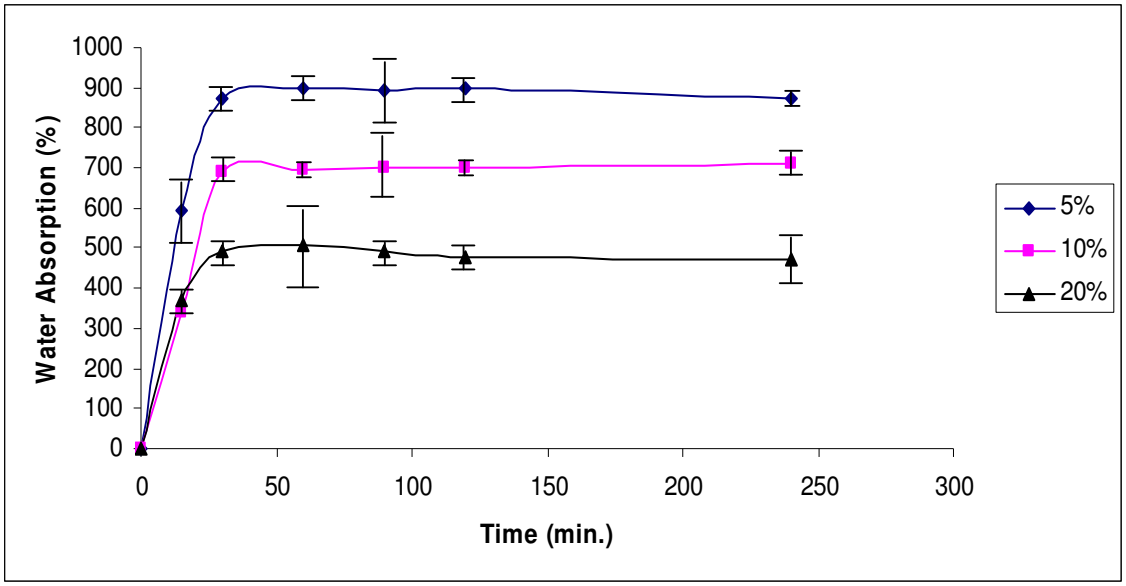

Figure 4.9. The effects of $CaCl_2.2H_2O$ concentration (5%, 10%, 20% w/v) on water uptake capacity of chitosan coated calcium alginate scaffolds.

As shown in this Figure, water uptake capacity decreased with increasing the crosslinker concentration. The water uptake ratios between 500% and 900% depending on $CaCl_2.2H_2O$ concentration were reached to the saturation values around 30 minutes. Minimum water uptake value (i.e. around 500%) was obtained at 20%(w/v) $CaCl_2.2H_2O$ (highest $CaCl_2.2H_2O$ concentration) because of the high degree of crosslinking of the scaffold shown in all cases a relatively small degree of

water uptake, apparently looking hydrophobic (Fundueanu et. al., 1998). As a result; when crossliker concentration increased, the crosslinking density increased, tight structure was formed, so the diffusion of water decreased and water absorption of the scaffold decreased (Mısırlı et al., 2005).

4.1.3.3. Effects of chitosan concentration on water uptake

The chitosan concentration was an effective parameter to determine the water absorption capacity of chitosan coated calcium alginate scaffolds in PBS at 37^0C. To investigate the effects of chitosan concentration on water uptake capacity of scaffold, three different chitosan (MMW) concentrations as 0.25%, 0.5% and 1.0% (w/v) were used for preparation of the scaffold. Other parameters were fixed as 20%(w/v) $CaCl_2.2H_2O$ concentration, 3%(w/v) sodium alginate concentration. The obtained results were summarized in Figure 4.10.

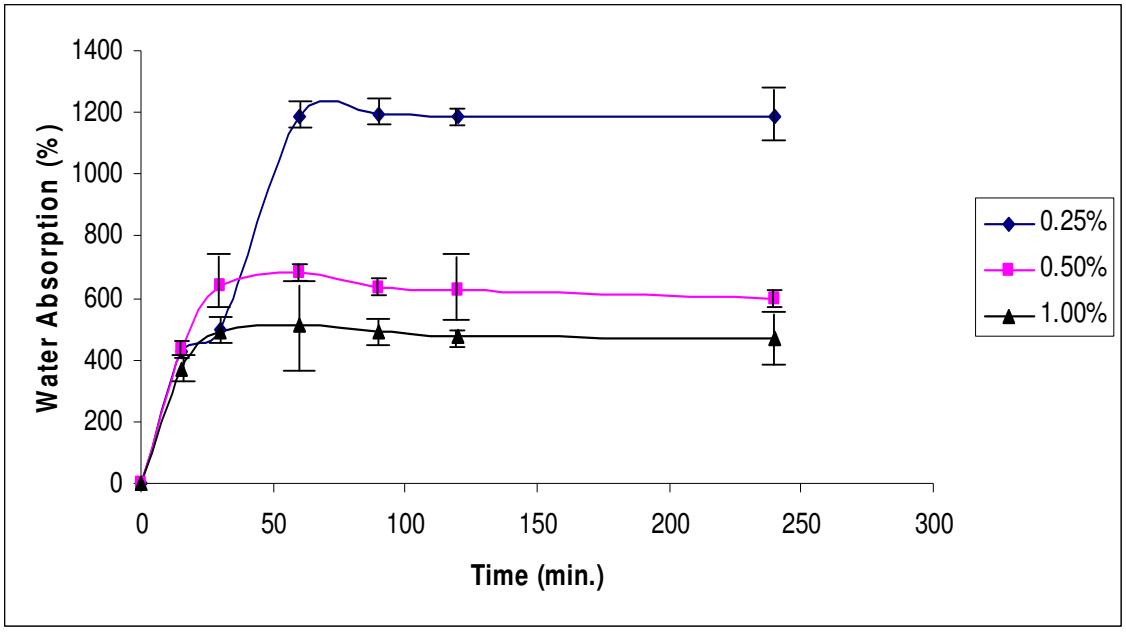

Figure 4.10. The effects of chitosan concentration (0.25%, 0.5%, 1% w/v) on water uptake capacity of chitosan coated calcium alginate scaffolds.

As shown in this Figure, water uptake capacity decreased with increasing the chitosan concentration. Water uptake capacity changed approximately between 500% and 1200% depending on chitosan concentration. Minimum water uptake value (i.e. around 200%) was observed at 1.00%(w/v) chitosan (highest chitosan

concentration) as expected. Alginate/chitosan polyelectrolyte complexes were formed by ionic crosslinking. When the chitosan concentration increased, the concentration of ammonium ion (NH_3^+) which interacted with carboxyl ion (COO^-) of alginate increased, and the tight and thick structure formed (Mısırlı et al., 2005). Because of that, the diffusion of buffer solution into the scaffold decreased. As a result, water uptake capacity decreased with increasing the chitosan concentration.

4.1.4. Hydrolysis/Degradation

We investigated the degradation behavior of chitosan coated calcium alginate scaffolds during certain periods of 13 weeks in PBS (pH: 7.4) with NaN_3 at 37^0C (Figure 4.11).

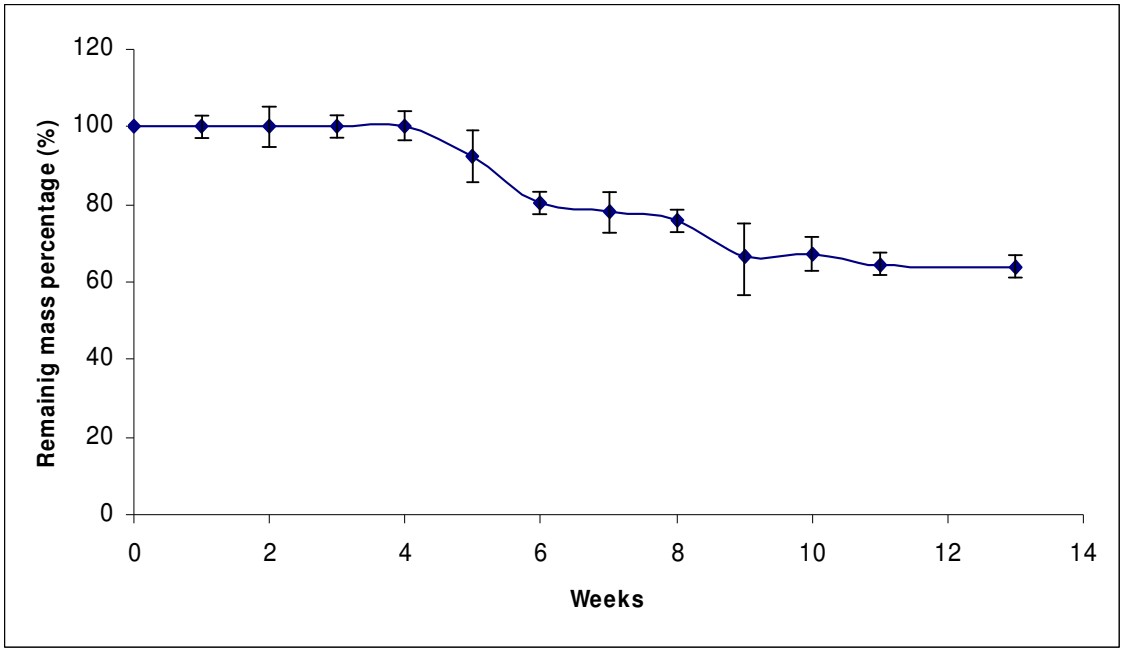

Figure 4.11. Gravimetric mass loss of chitosan coated calcium alginate scaffold during 13 weeks in PBS (pH: 7.4) with NaN_3 at 37^0C.

Any mass degredation was not observed during 1 month. Although many natural biopolymers degrade quickly in an aqueous environment, throughout the 1-month period tested the chitosan coated calcium alginate scaffolds showed no signs of degradation. Because alginate firstly crosslinked with 20% $CaCl_2.2H_2O$ then 1% chitosan (MMW). After 1 month, we observed sligthly decrease in weigth of scaffold. Biodegradable nerve guides gradually degrade, with a minimal foreign body reaction.

The mass loss of the scaffolds was about 33% in the degredation period in PBS (pH: 7.4) with NaN_3 at 37^0C. Studies have demonstrated that the use of a slowly degradable polymeric nerve guide can improve the nature and rate of nerve regeneration across a short gap in small nerves (den Dunnen et al., 2000; Matsumoto et al., 2000; Evans et al., 1999; Aldini et al., 1996).

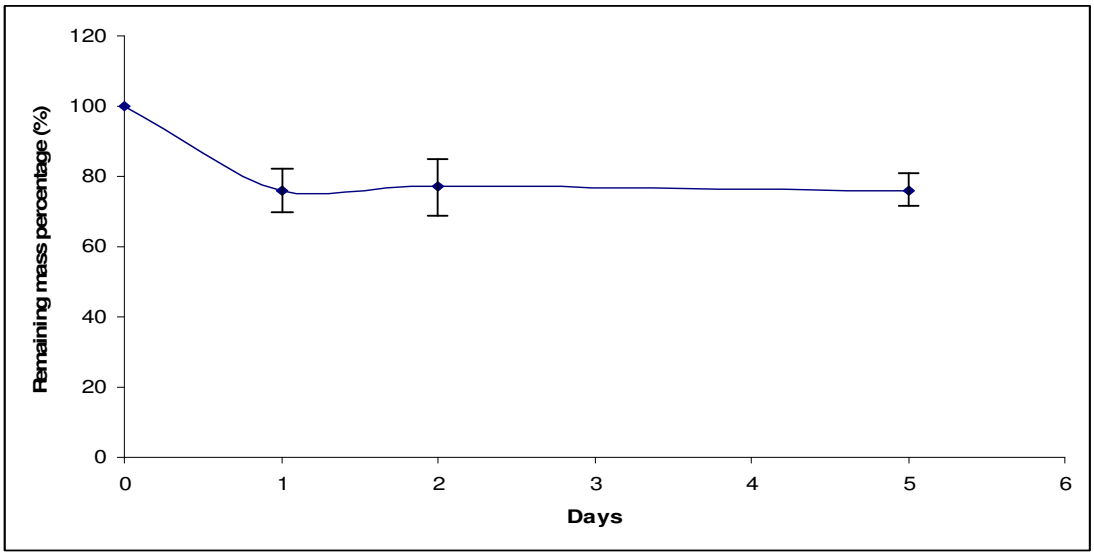

Figure 4.12. Gravimetric mass loss of chitosan coated calcium alginate scaffold during 5 days in culture medium at 37^0C.

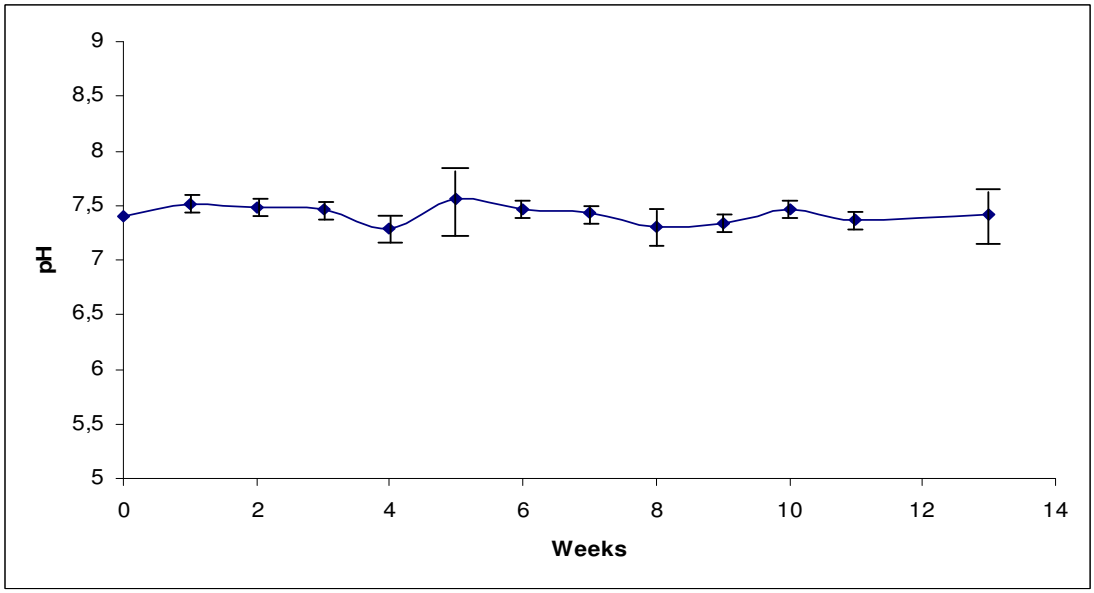

Figure 4.13. pH changes in chitosan coated calcium alginate scaffold during 13 weeks in PBS (pH: 7.4) with NaN_3 at 37 ^{o}C.

We studied in culture medium for cell attachment study and MTT assay. So that, we wanted to see that what is the degradation profile of the scaffold in certain periods of 5 days in culture medium at 37^0C (Figure 4.12). The mass loss of the scaffolds was about 25% in the degredation period.

pH changes were also evaluated weekly during the degradation period in PBS (pH: 7.4) with NaN_3 at 37^0C. As evidenced in Figure 4.13, there was no drastic change in pH during 13 weeks.

4.1.5. Permeability studies

Permeability properties of chitosan coated calcium alginate scaffold were examined because of literature says “The degree of permeability of the nerve guide may also influence nerve regeneration” (Rodriguez et al., 1999). The permeability of different molecules like carbohydrate and protein ranging from molecular weight 180–66,000 Da across the chitosan coated calcium alginate scaffolds was studied in PBS (pH:7.4) at 37^0C and depicted in Figure 4.14.

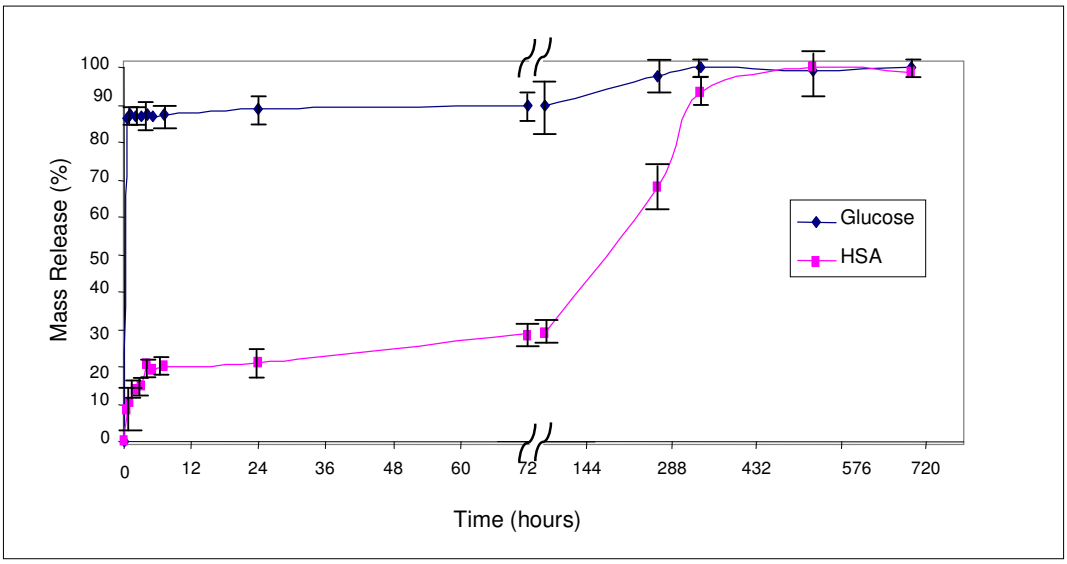

Figure 4.14. Permeability of glucose and HSA across chitosan coated calcium alginate scaffold over time in PBS of pH 7.4 at 37^0C.

The permeability of the scaffold has been evaluated by studying the diffusion of glucose and HSA molecules from a saturated solution trapped inside a scaffold to the external medium. The optical density measured increased gradually until the

equilibrium between the internal and external solution concentrations was reached (Figure 4.14). The diffusion rate of glucose molecules and HSA molecules are different, because of molecular weigth. The diffusion rate of glucose molecules are faster than HSA molecules. The size of the tube wall porous and its stability over time are important factors to determine the flow of different constituents that may promote or inhibit regeneration. Glucose molecules reached the saturation value nearly 30 minutes but HSA molecules reach the saturation value nearly 336 hours (14 days). The diffusion of HSA across the chitosan coated calcium alginate scaffold is slow (336 h until equilibrium) but there is no any preventative effect for HSA diffusion across the chitosan coated calcium alginate scaffold. This result show that, nerve guide is free of pores.

These results suggest that molecules or tropic factors of the size of HSA could diffuse freely across the scaffold. It was reported that an increase in permeability of conduits improves axonal regeneration (Jenq et al., 1993; Kim, et al., 1993). The favorable effects of permeable tubes may be attributed to different reasons such as: metabolic exchange across the tube wall, diffusion into the guide lumen of growth promoting factors generated in the external environment, retention of trophic factors secreted by the nerve stumps, or a combination of all these (Aebischer et al., 1988).

4.1.6. Mechanical testing

The mechanical strength of dry and wet scaffolds was studied to ensure that the scaffolds could withstand suturing and remain intact after surgery. We observed the effect of the crosslinking process onto the mechanical properties of the alginate scaffold in dry and wet form. In dry form, the young's modulus (E-modulus) values of alginate, calcium alginate and chitosan coated calcium alginate scaffols were found to be 7771.66, 13139.39, and 7555.37 respectively. These results show that the brittleness of alginate scaffold was increased after crosslinking with $CaCl_2.2H_2O$. After coating the calcium alginate scaffold with chitosan, the brittleness of the scaffold decreased. The tensile strength (Rm) values of alginate, calcium alginate and chitosan coated calcium alginate scaffolds were found to be 31.01, 12.88, and 63.98, respectively. Tensile strength of alginate scaffolds decreased with crosslinking of the alginate scaffold with $CaCl_2.2H_2O$, while elongation increased. Tensile strength of the

calcium alginate scaffolds increased with coating the calcium alginate with chitosan, while elongation decreased.

Table 4.1. Mechanic strength results of dry and wet form of scaffols.

Dry Form

	E-Modulus	Rm	ε Fmax.
Sample	(N/mm^2)	(N/mm^2)	%
Alginate	7771.66	31.01	1.16
Calcium Alginate	13139.39	12.88	1.67
Chitosan Coated Calcium Alginate	7555.37	63.98	2.39

Wet Form

	E-Modulus	Rm	ε Fmax.
Sample	(N/mm^2)	(N/mm^2)	%
Calcium Alginate	3884.69	20.55	3.93
Chitosan Coated Calcium Alginate	484.78	38.68	6.67

In wet form, E-modulus values were decreased after water interaction of the scaffolds. This result showed that water uptake induced ductile form in all scaffold formulation. Water is known to be a very effective plasticizer for most biopolymers (Slade &Levine, 1991) and its plasticizing action is reflected in lowering of the fracture strength, elastic modulus and increasing of flexibility of the film (Biliaderis et al., 1999; Chang et al., 2000; Chang et al., 2006; Diab et al., 2001; Kalichevsky et al., 1993; Kristo et al., 2007; Lazaridou & Biliaderis, 2002; Lazaridou et al, 2003; Ollett et al., 1991; van Soest et al., 1996). The tensile strength (Rm) values of calcium alginate scaffolds and chitosan coated calcium alginate scaffolds were found to be 20.55, and 38.68, respectively. Tensile strength of calcium alginate scaffolds decreased with crosslinking of the calcium alginate scaffolds with chitosan, while elongation increased. Presence of the chitosan in scaffold structure decreased the E-modulus values or in other word decreased the brittleness of the calcium alginate in two forms (wet and dry).

4.1.7. Blood Compatibility

In recent years, various biomaterials that are natural or synthetic have been widely used for manufacturing biomedical applications including artificial organs, medical devices, and disposable clinical apparatus (Ishihara et al., 1999), such as nerve guides, vascular prostheses, blood pumps, artificial kidney, heart valves, pacemaker

lead wire insulation, intra-aortic balloon, artificial hearts, dialyzers and plasma separators, which could be used in contact with blood. However, the polymers presently used are conventional materials, such as cellulose, chitosan, poly (tetrafluoroethylene) (PTFE), segmented polyetherurethane (SPU), polyethylene (PE), poly (vinyl chloride) (PVC), silicone rubber (SR), nylon and polysulfone (PSf) (Mao et al., 2004). Before use, all biomaterials must be evaluated depending on criteria such as biocompatibility. To evaluate the biocompatibility of scaffold, cell and compatibility tests were made. Material biocompatibility is generally considered to have close relation with protein adsorption process, because adsorbed proteins may trigger the coagulation sequence (Mao et al., 2004). A rapid adsorption of plasma proteins occurs when a foreign material is brought into contact with the blood. The plasma are said to be mainly albumin, γ-globulin, fibrinogen and prothrombin. It has been reported elsewhere that fibrinogen is a major part of the adsorbed protein layer.

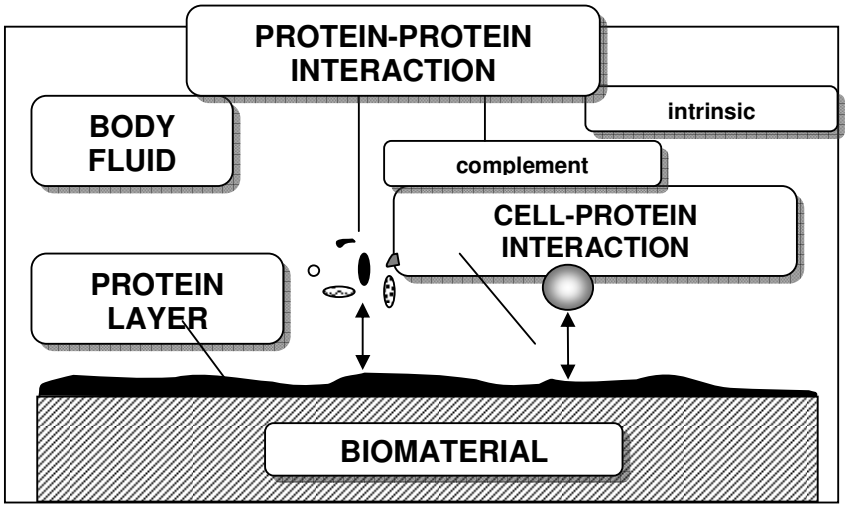

Figure 4.15. The role of adsorbed proteins in body fluid biomaterial interaction.

When biomaterials in use come into contact with blood, first small molecules (e.g. water molecules and ions) reach to the surface which may or may not be adsorbed. This is followed by plasma protein adsorption. The first protein layer adsorbed on the biomaterial surface determines the subsequent events of the coagulation cascade (via the intrinsic pathway), and the complement activation as shown in Figure 4.15. (via the intrinsic-extrinsic pathways) (Denizli, 1999).

Generally, two main strategies are being followed for improving haemocompatibility of biomaterials (Mao et al., 2004) :

1. To create surfaces that prevents or suppresses unwanted or uncontrolled reactions of the blood (e.g. activation of the blood coagulation cascade, or activation and aggregation of adherent blood platelets).
2. To prepare polymers those are inert or passive with respect to blood reactions.

4.1.7.1. *In vitro* haemocompatibility tests

In this study, we crosslinked the alginate with $CaCl_2.2H_2O$ and chitosan, respectively. We evaluated the blood compatibilty of alginate, calcium alginate and chitosan coated calcium alginate scaffolds by carring out the activated partial thromboplastin time (APTT), thrombin time (TT), fibrinogen time and protrombin time (PT) tests, in vitro. APTT tests exhibit the bioactivity of intrinsic blood coagulation factors and PT test relates to extrinsic blood coagulation factors on biomaterial surface.

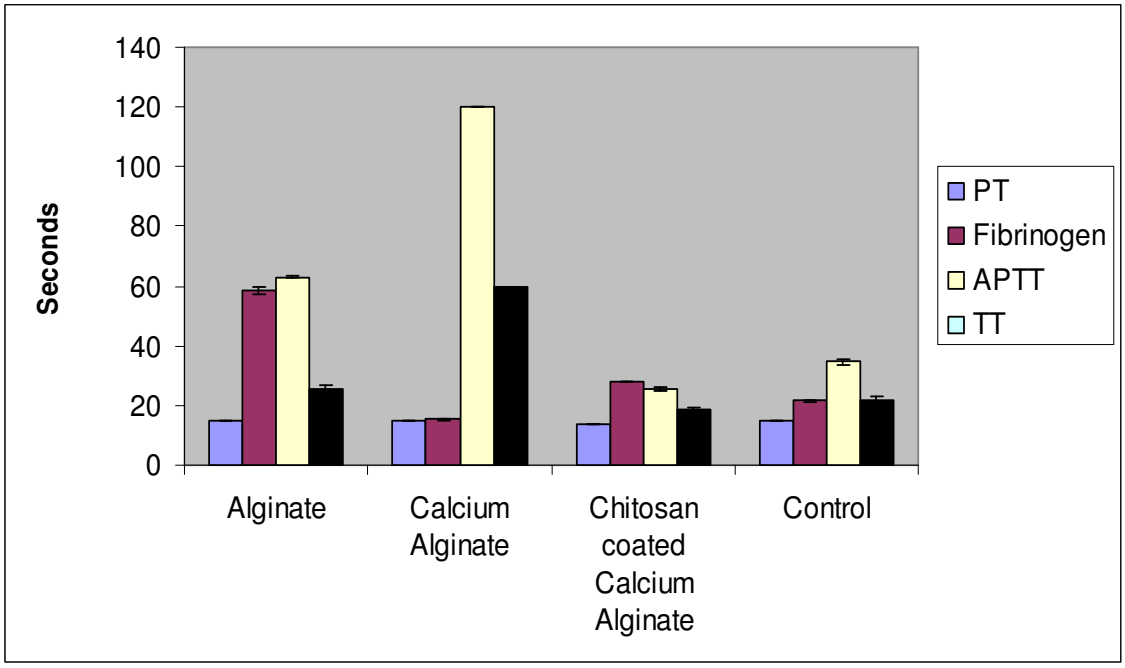

Figure 4.16. Coagulation times of human plasma (reported in sec).

Thrombin Time (TT) is a coagulation assay which is usually performed in order to detect for the therapeutic level of the anticoagulant Heparin. Figure 4.16 summarizes

the TT, Fibrinogen, APTT and PT data obtained in these tests. As seen in this Figure, all the APTT, TT, fibrinogen time and PT values for chitosan coated calcium alginate scaffolds are in range of the standard. But all APTT, TT, fibrinogen time and PT values for alginate and calcium alginate scaffolds aren't in range of the standard (Figure 4.16). So we can say that the chitosan improve the blood compatibility of alginate and calcium alginate scaffolds. Alginate and calcium alginate scaffolds are not blood compatible materials but after interaction of calcium alginate scaffolds with chitosan, blood compatible materials were obtained because chitosan has both reactive amino and hydroxyl groups, which can be used to chemically alter alginate properties under mild reaction conditions. Chitosan exhibits properties that make it desirable candidate for biocompatible and blood-compatible biomaterials (Popowicz et al., 1985; Chuang et al., 1999).

4.1.8. Biocompatibility

4.1.8.1. Cell attachment study

The cell attachment study as a part of biocompatibility tests were examined with fibroblast cells. The capacity of cellular adhesion of the L-929 mouse fibroblast cells on the chitosan coated alginate scaffolds was tested at incubation periods of 48 h.

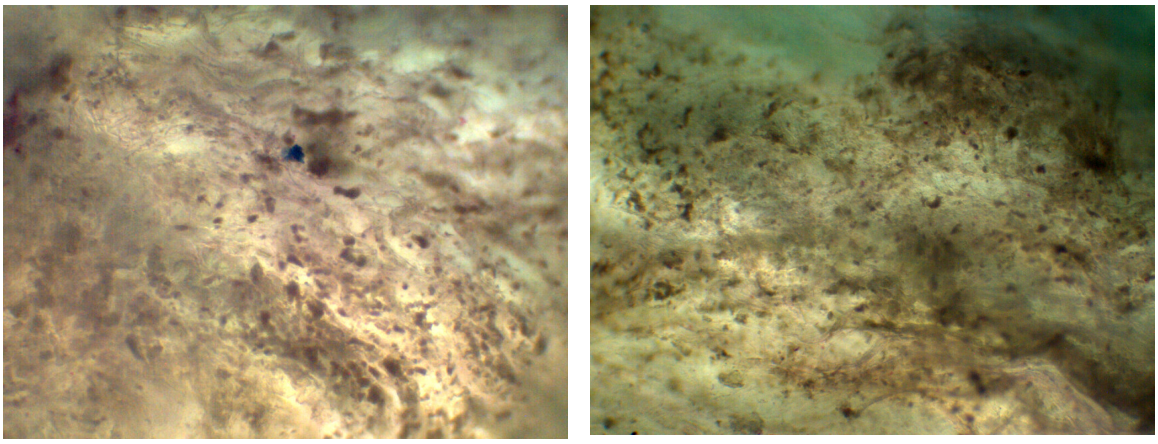

Figure 4.17. Optic micrographs of L-929 on the scaffold.

In this study; fibroblast cells were easily attached, spread and growth over these

scaffolds (Figure 4.17). As a result, good cell proliferation of L-929 cells on chitosan coated calcium alginate scaffolds was observed.

4.1.8.2. MTT assay

Cell attachment, spreading and migration on substrates are the first sequential reactions when coming into contact with a material surface, which is crucial to cell survival (Tao et al., 2007). The cellular behavior on biomaterial is an important factor for evaluation of its biocompatibility. Figure 4.18 shows the fibroblasts morphology in the vicinity of chitosan coated calcium alginate scaffolds after culturing. It is clearly found that the fibroblasts have normal morphology when compared to the negative control after 48 h. co-culture, and there is a good cell adhesion.

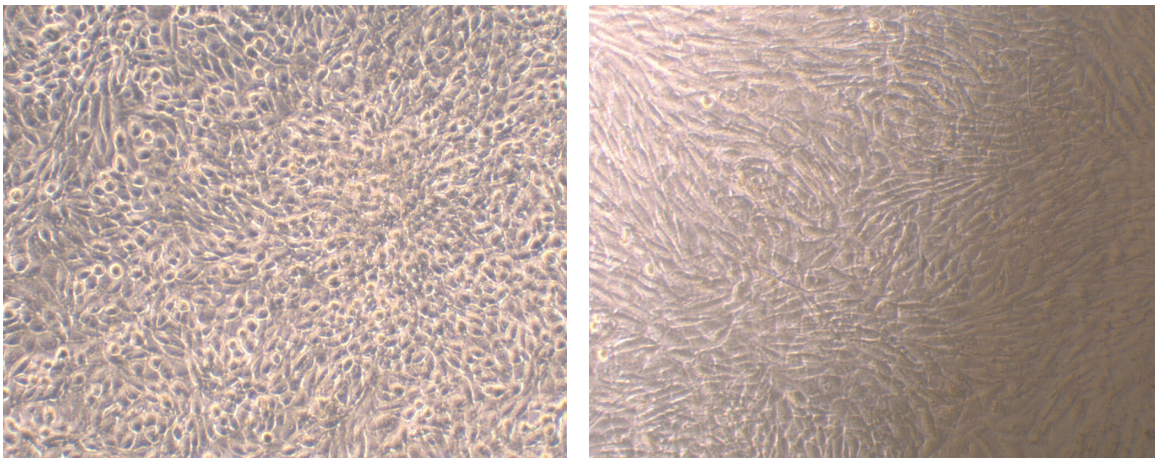

(a) **(b)**

Figure 4.18. Optic micrographs of (a) L-929 without scaffold (b) L-929 with scaffold.

Cell viability results obtained in fibroblasts with MTT assay are depicted in Fig. 4.19. The viabilities values obtained for chitosan coated calcium alginate scaffolds from 100% to 95%. Results show that chitosan coated calcium alginate scaffolds show a weak cytotoxicity in 72 h., and 96 h. incubation time, caused by the surrounding condition. Fortunately, this very weak cytotoxicity cannot influence the body metabolism and can be accepted in medical applications. As a results: chitosan coated calcium alginate scaffolds don't have any cytotoxic effect or in other word don't inhibit cell proliferation.

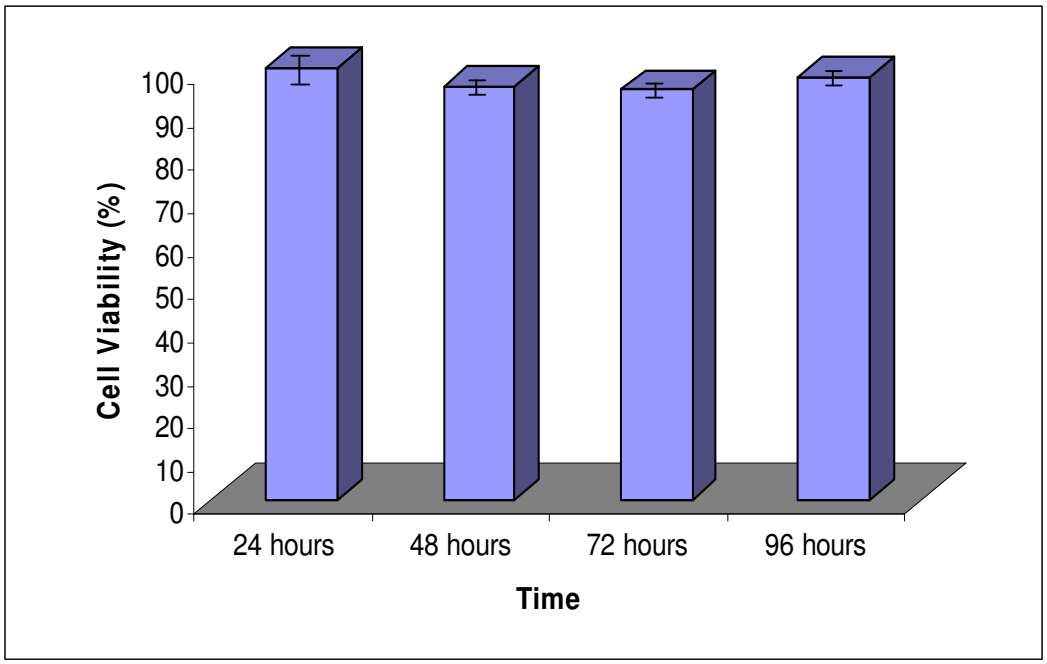

Figure 4.19. Cell viability graph of scaffold.

5. CONCLUSION

In the presented study, biopolymeric scaffolds were prepared by freeze-dry method as a nerve guide. The direction of growth and size of the ice crystals are a function of the temperature gradient, linear, radial, and/or random pore directions and sizes can be produced with freeze-dry methodology. We prepared the nerve guide with alginate and crosslinked the alginate scaffolds with calcium and coated the calcium alginate scaffolds with chitosan to improve the mechanic strength, blood compatibility and biocompatibility. Chitosan has unique polymeric cationic character which combines with the electronegative groups on the cell surface, which may benefit cell adhesion, spread, and growth (Ao et al., 2005). Water uptake capacity of chitosan coated calcium alginate scaffold changed between 500% to 2000%. Formulation which will be used as a nerve guide has 500% water uptake capacity. A nerve guide with 500% water uptake capacity which reported in literature was potentially support axonal regenaration after nervous system injury (Stokols et al., 2004). Chitosan coated calcium alginate scaffold has slow degradation profile. Studies have demonstrated that the use of a slowly degradable polymeric nerve guide can improve the nature and rate of nerve regeneration across a short gap in small nerves (den Dunnen et al., 2000; Matsumoto et al., 2000; Evans et al., 1999; Aldini et al., 1996). The scaffolds are permeable to glucose and HSA molecules and exhibit good cytocompatibility with the cells. As a result; freeze-dried chitosan coated calcium alginate scaffolds created in this study have a number of favorable properties for potentially supporting axonal regeneration after nervous system injury.

6. REFRENCES

Aebischer, P., GueHnard, V., Winn, S.R., Valentini, R.F., Galletti, P.M., 1988, Blind-ended semipermeable guidance channels support peripheral nerve regeneration in the absence of a distal nerve stump. Brain Res. 454:179}87.

Aldini, N.N., Perego, G., Cella, G.D., Maltarello, M.C., Fini, M., Rocca, M., Giardino, R., 1996, Effectiveness of a bioabsorbable conduit in the repair of peripheral nerves. Biomaterials, 17:959–62.

Ao, Q., Wang, A., Cao W., Zhao, C., Gong, Y., Zhao N., 2005, Fabrication nd characterization of chitosan nerve conduits with microtubular architectures, Tsinghua Sci. And Tech. 10 (4):435–8.

Araki, T., Milbranth, J., 1996, Ninjurin, a novel adhesion molecule, is induced by nerve injury and promotes axonal growth. Neuron, 17:353-61.

Barres, B.A., Jacobson, M.D., Schmid, R., Sendtner, M., Raff, M.C., 1993, Does oligodendrocyte survival depend on axons?" Curr. Biol., 3:489–97.

Berger, A., Lassner, F., Schaller, E., 1994, The Dellon tube in injuries of peripheral nerves. Handchirurgie, Mickrochirurgie, Plastische Chirurgie 26:44–7.

Biliaderis, C.G., Lazaridou, A., & Arvanitoyannis, I., 1999, Glass transition and physical properties of polyol-plasticized pullulan-starch blends at low moisture. Carbohydrate Polymers, 40, 29–47.

Chandy, T., Sharma, C.P., 1990, Chitosan as a biomaterial. Biomat. Art. Cells Art. Org. 18:1}24.

Chang, Y.P., Cheah, P.B., & Seow, C.C., 2000, Plasticizing–antiplasticizing effects of water on physical properties of tapioca starch films in the glassy state. Journal of Food Science, 65, 445–451.

Chang, Y.P., Abd Karim, A., & Seow, C.C., 2006, Interactive plasticizing–antiplasticizing effects of water and glycerol on the tensile properties of tapioca starch films. Food Hydrocolloids, 20, 1–8.

Chen, L.E., Seaber, A.V., Urbaniak, J.R., Murrell, G.A., 1994, Denatured muscle as a nerve conduit: a functional, morphologic, and electrophysiologic evaluation. J Reconstr Microsurg, 10:137–44.

Chen, Y.S., Chang, J.Y., Cheng, C.Y., Tsai, F.J., Yao, C.H, Liu, B.S., 2005, An in vivo evaluation of a biodegradable genipin-cross-linked gelatin peripheral nerve guide conduit material. Biomaterials 26:3911–3918.

Chuang, W.Y., Young, T.H., Yao, C.H., et al.,1999, Properties of the poly(vinyl alcohol)/chitosan blend and its effect on the culture of fibroblast in vitro. Biomaterials, 20:16, 1479-1487.

Coleman M.P., Conforti L., Buckmaster, A.E., Tarlton, A., Ewing, R.M., Brown, M.C., Lyon, M.F., Perry, V.H., 1998, An 85-kb Tandem Triplication in the Slow Wallerian Degeneration (Wld s) Mouse, Proceedings of the National Academy of Sciences of the United States of America, Vol. 95, No. 17., pp. 9985-9990.

Coleman, M.P., Conforti, L., Buckmaster, E.A., Tarlton, A., Ewing, R.M., et al., 1998, An 85-kb tandem triplication in the slow Wallerian degeneration (Wlds) mouse." Proc. Natl. Acad. Sci. USA, 95:9985–90.

Dailey, A.T., Avellino, A.M., Benthem, L., Silver, J., Kliot, M., 1998, Complement depletion reduces macrophage infiltration and activation during Wallerian degeneration and axonal regeneration. J. Neurosci., 18:6713–22.

den Dunnen, W.F., Meek, M.F., Grijpma, D.W., Robinson, P.H., Schakenraad, J.M., 2000, In vivo and in vitro degradation of poly [50/50(85/15)LA/e-CL], and the implications for the use in nerve reconstruction. J. Biomed. Mater. Res. 51:575–85.

Diab, T., Biliaderis, C.G., Gerasopoulos, D., & Sfakiotakis, E., 2001, Physico-chemical properties and application of pullulan edible films and coatings in fruit preservation. Journal of Science of Food and Agriculture, 81, 988–1000.

Domard, A., Varum, K.M., Roberts, G.A.F., 1998, Advances in chitin science, vol. II. France: Jacques AndreHpress.

Evans, G.R.D., Brandt, K., Widmer, M.S., Lu, L., Meszlenyi, R.K., Guptac, P.K., Mikos, A.G., Hodges, J., Williams, J., Gurlek, A., Nabawi, A., Lohman, R., Patrick, Jr. C.W., 1999, In vivo evaluation of poly(l-lactic acid) porous conduits for peripheral nerve regeneration. Biomaterials, 20:1109–15.

Fields, R.D., Le Beau, J.M., Longo, F.M., Ellisman, M.H., 1989, Nerve Regeneration through artificial tubular implants. Prog Neurobiol., 33:87–134.

Fundueanu, G., Esposito, E., Mihai, D., Carpov, A., Desbrieres, J., Rinaudo, M., Nastruzzi, C., 1998, Preparation and characterization of Ca-alginate microspheres by a new emulsification method. International Journal of Pharmaceutics, 170;11–21.

Geller, H.M., Fawcett, J.W., 2002, Building a bridge: engineering spinal cord repair. Exp Neurol., 174(2):125–36.

George, R., Griffin, J.W., 1994, Delayed macrophage responses and myelin clearance during Wallerian degeneration in the central nervous system: the dorsal radiculotomy model. Exp. Neurol., 129:225–36.

Gohel, M.C., Amin, A.F., 1998, Formulation optimization of controlled release diclofenac sodium microspheres using factorial design. Journal of Controlled Release, 51:115– 122.

Guertin, A.D., Zhang, D.P., Mak, K.S., Alberta, J.A., Kim, H.A., 2005, Microanatomy of axon/glial signaling duringWallerian degeneration. Jouranl of Neuroscience, 25:3478–87.

Hadlock, T., Sundback, C., Koka, R., Hunter, D., Cheney, M., Vacanti, J., 1999, A novel, biodegradable polymer conduit delivers neurotrophins and promotes nerve regeneration. Laryngoscope, 109(9):1412–6.

He, Z., Koprivica, V., 2004, The Nogo signaling pathway for regeneration block. Annu. Rev. Neurosci., 27:341–68.

Heumann, R., Korsching, S., Bandtlow, C., Thoenen, H., 1987, Changes of nerve growth factor synthesis in nonneuronal cells in response to sciatic nerve transection. J. Cell Biol., 104:1623–31.

IJkema-Paassen, J., Jansen, K., Gramsbergen, A., Meek, M.F., 2004, Transection of peripheral nerves, bridging strategies and effect evaluation, Biomaterials 25;583–1592.

Ishihara, K., Ishikawa, E., Iwasaki, Y., Nakabayashi, N., 1999, Inhibition of fibroblast cell adhesion on substrate by coating with 2-methacryloyloxyethyl phosphorylcholine polymers. Journal Of Biomaterials Science-Polymer Edition, 10:10, 1047-1061.

Jansen, K., van der Werff, J.F.A., van Wachem, P.B., Nicolai, J-P.A., de Leij, L.F.M.H., van Luyn, M.J.A., 2004, A hyaluronan-based nerve guide: in vitro cytotoxicity, subcutaneous tissue reactions, and degradation in the rat. Biomaterials, 25:483–489.

Jenq, C-B, Coggeshall, R.E., 1987, Permeable tubes increase the length of the gap that regenerating axons can span. Brain Res., 408:239–42.

Kalichevsky, M.T., Blanshard, J.M.V., & Tokarczuk, P.F., 1993, Effect of water content and sugars on the glass transition of casein and sodium caseinate. International Journal of Food Science and Technology, 28:139–151.

Keeley, R.D., Nguyen, K.D., Stephanides, M.J., Padilla, J., Rosen, J.M., 1991, The artificial nerve graft: a comparison of blended elastomerhydrogel elastomerhydrogel with polyglycolic acid conduits. J Reconstr Microsurg, 7:93–100.

Kerschensteiner, M., Schwab, M.E., Lichtman, J.W., Misgeld, T., 2005, In vivo imaging of axonal degeneration and regeneration in the injured spinal cord. Nat. Med. 11:572–77.

Kim, D.H., Connolly, S.E., Zhao, S., Beuerman, R.W., Voorhies, R.M., Kline, D.G., 1993, Comparison of macropore, semipermeable, and nonpermeable collagen conduits in nerve repair. J Reconstr Microsurg., 9:415–20.

Koshinaga, M., Whittemore, S.R., 1995, The temporal and spatial activation of microglia in fiber tracts undergoing anterograde and retrograde degeneration following spinal cord lesion. J. Neurotrauma, 12:209–22.

Kristo, E., Biliaderis, C.G., & Zampraka, A., 2007, Water vapor barrier and tensile properties of composite caseinate–pullulan films: Biopolymer composition effects and impact of beeswax lamination. Food Chemistry, 101:753–764.

Lazaridou, A., & Biliaderis, C.G., 2002, Thermophysical properties of chitosan, chitosan–starch and chitosan–pullulan films near the glass transition. Carbohydrate Polymers, 48:179–190.

Lazaridou, A., Biliaderis, C.G., & Kontogiorgos, V., 2003, Molecular weight effects on solution rheology of pullulan and mechanical properties of its films. Carbohydrate Polymers, 52:151–166.

Lin, A.S., Barrows, T.H., Cartmell, S.H., Guldberg, R.E., 1993, Microarchitectural and mechanical characterization of oriented porous polymer scaffolds. Biomaterials, 24(3):481–9.

Lindholm, D., Heumann, R., Hengerer, B., Thoenen, H., 1988, Interleukin 1 increases stability and transcription of mRNA encoding nerve growth factor in cultured rat fibroblasts. J. Biol. Chem., 263:16348–51.

Liu, H.M., Yang, L.H., Yang, Y.J., 1995, Schwann cell properties: 3. C-fos expression, bFGF production, phagocytosis and proliferation during Wallerian degeneration. J. Neuropathol. Exp. Neurol., 54:487–96.

Ludwin, S.K., 1990, Oligodendrocyte survival in Wallerian degeneration." Acta Neuropathol., 80:184–91.

Mao, S.R., Shuai, X.T., Unger, F., Simon, M., Bi, D.Z., Kissel, T., 2004, The depolymerization of chitosan: effects on physicochemical and biological properties. Internatıonal Journal Of Pharmaceutıcs, 281:1-2, 45-54.

Mack, T.G., Reiner, M., Beirowski, B., Mi, W., Emanuelli, M., et al., 2001, Wallerian degeneration of injured axons and synapses is delayed by a Ube4b/Nmnat chimeric gene. Nat. Neurosci., 4:1199–206.

Mackinnon, S.E., Dellon, A.L., Hudson, A.R., Hunter, D.A., 1984, Chronic nerve compression-an experimental model in the rat. Ann Plast Surg.,13:1 12–20.

Madihally, S.V., Matthew, H.W., 1999, Porous chitosan scaffolds for tissue engineering. Biomaterials, 20(12):1133–42.

Matsumoto, K., Ohnishi, K., Kiyotani, T., Sekine, T., Ueda, H., Nakamura, T., Endo, K., Shimizu, Y., 2000, Peripheral nerve regeneration across an 80-mm gap bridged by a polyglycolic acid (PGA)-collagen tube filled with laminin-coated collagen fibers: a histological and electrophysiological evaluation of regenerated nerves. Brain Res., 868:315–28.

Matsumoto, K., Ohnishi, K., Sekine, T., Ueda, H., Yamamoto, Y., Kiyotani, T., Nakamura, T., Endo, K., Shimizu, Y., 2000, Use of a newly developed artificial nerve conduit to assist peripheral nerve regeneration across a long gap in dogs. Asaio J., 46: 415–20.

Merle, M., Dellon, A.L., Campbell, J.N., Chang, P.S., 1989, Complications from silicon-polymer intubulation of nerves. Microsurgery, 10:130–3.

Mısırlı, Y., Ozturk, E., Kursaklioglu, H., Denkbas, E.B., 2005, Preparation and characterization of mitomycin-C loaded chitosan-coated alginate microspheres for chemoembolization. Journal of Microencapsulation, 22:167–178.

Miller, G.L., 1959, Use of dinitrosalicylic acid reagent for determination of reducing sugar. Analytical Chemistry., 31:426–428.

Mosmann, T., 1983, Rapid colorimetric assay for cellular growth and survival: application to proliferation and cytotoxicity assays. J Immunol Methods. 16;65(1-2):55-63.

Murinson, B.B., Archer, D.R., Li, Y., Griffin, J.W., 2005, Degeneration of myelinated efferent fibers prompts mitosis in Remak Schwann cells of uninjured C-fiber afferents. Journal of Neuroscience, 25:1179–87.

Muzzarelli, R.A.A., Jeuniaux, C., Gooday, G.W.(Eds.), 1986, Chitin in Nature and Technology, Plenum, New York.

Olabarrieta, I., Forsstro, Èm D., Gedde, U.W., Hedenqvist, M.S., 2001, Transport properties of chitosan and whey blended with poly(ε-caprolactone) assessed by standard permeability measurements and microcalorimetry. Polymer 42:4401-4408.

Ollett, A.L., Parker, R., & Smith, A.C., 1991, Deformation and fracture behaviour of wheat starch plasticized with glucose and water. Journal of Materials Science, 26:1351–1356.

Pˆego, A.P., Poot, A.A., Grijpma, D.W., Feijen, J., 2003, Biodegradable elastomeric scaffolds for soft tissue engineering. Journal of Controlled Release, 87:69–79.

Perry, V.H., Brown, M.C., Tsao, J.W.,1992, The effectiveness of the gene which slows the rate of wallerian degeneration in c57bl/ola mice declines with age. Eur J Neurosci., 4:1000–1002.

Popowıcz, P., Kurzyca, J., Dolınska, B., et al., 1985, Cultivation of mdck epithelial-cells on chitosan membranes. Biomedica Biochimica Acta, 44:2, 1329-1333.

Rajaonarivoi, M., Vauthier, Y.C., Couarraze, G., Puisieux, F., Couvreur, P., 1993, Development of a new drug carrier made from alginate. J. Pharm. Sci., 82(9), 912–917.

Ribeiro, A.J., Neufeld, R.J., Arnaud, P., Chaumeil, J.C., 1999, Microencapsulation of lipophilic drugs in chitosan-coated alginate microspheres. International Journal of Pharmaceutics, 187:115–123.

Rodriguez, F.J., Gomez, N., Perego, G., Navarro, X., 1999, Highly permeable polylactide-caprolactone nerve guides enhance peripheral nerve regeneration through long gaps. Biomaterials, 20:1489-1500.

Rosner, B.I., Siegel, R.A., Grosberg, A., Tranquillo, R.T., 2003, Rational design of contact guiding, neurotrophic matrices for peripheral nerve regeneration. Ann Biomed Eng., 31:1383–401.

Schmidt, C.E., Leach, J.B., 1993, Neural tissue engineering: strategies for repair and regeneration. Annu Rev Biomed Eng., 5:293–347.

Slade, L., & Levine, H., 1991, Beyond water activity: Recent advantages based on an alternative approach to the assessment of food quality and safety. Critical Reviews in Food Science and Nutrition, 30:115–360.

Soest, J.J.G., de Wit, D.J.F., & Vliegenthart, G., 1996, Mechanical properties of thermoplastic waxy maize starch. Journal of Applied Polymer Science, 61:1927–1937.

Stokols, S., Tuszynski, M.H., 2004, The fabrication and characterization of linearly oriented nerve guidance scaffolds for spinal cord injury. Biomaterials 25:5839–5846.

Tang, J.B., Shi, D., Zhou, H., 1995, Vein conduits for repair of nerves with a prolonged gap or in unfavourable conditions: an analysis of three failed cases. Microsurgery, 16:133–7.

Tao, H., Cheng-lin, C., Li-hang, Y., Yao-pu, P., et al., 2007, *In vitro* biocompatibility of titanium-nickel alloy with titanium oxide film by H202 oxidation. Trans. Nonferrous Met. Soc. China, 17:553-557.

Thomas, P.K., King, R.H., 1974, The degeneration of unmyelinated axons following nerve section: an ultrastructural study. J. Neurocytol., 3:497–512.

Turner, J.E., Glaze, K.A., 1976, The early stages of Wallerian degeneration in the severed optic nerve of the Newt (Triturus viridescens)". Anat. Rec., 187:291–310.

Vargas, M.E., Singh, S.J., Barres, B.A., 2005, Why is Wallerian degeneration so slow in the CNS. Soc. Neurosci., Program No. 439.2.

Vargas, M.E., Barres, B. A., 2007, Why is Wallerian Degeneration in the CNS so slow. Annual Review of Neuroscience, 30:153-79.

Verreck, G., Chun, I., Li, Y., Kataria, R., Zhang, Q., Rosenblatt, J., Decorte, A., Heymans, K., Adriaensen, J., Bruining, M., Remoortere M. V., Borghys, H.,

Meert, T., Peeters, J., Brewster, M.E., 2004, Preparation and physicochemical characterization of biodegradable nerve guides containing the nerve growth agent sabeluzole. Biomaterials, 26:1307–1315.

Waller, A., 1850, Experiments on the section of the glossopharyngeal and hypoglossal nerves of the frog, and observations of the alterations produced thereby in the structure of their primitive fibres. Philos. Trans. R. Soc., 140:423–29.

Wang, K.K., Costas, P.D., Bryan, D.J., Eby, P.L., Seckel, B.R., 1995, Inside-out vein graft repair compared with nerve grafting for nerve regeneration in rats. Microsurgery, 16:65–70.

Wang, K.K., Cetrulo, Jr. C.L., Seckel, B.R., 1999, Tubulation repair of peripheral nerves in the rat using an inside-out intestine sleeve. J. Reconstruct Microsurg, 15:547–54.

Xu, X., Yu, H., Gao, S., Mao, H-Q., Leong, K.W., Wang, S., 2002, Polyphosphoester microspheres for sustained release of biologically active nerve growth factor. Biomaterials, 23: 3765–72.

Xu, X., Yee, W.C., Hwang, P.Y.K., Yu, H., Wan, A.C.A., Gao, S., Boon, K.L., Mao, H-Q., Leong, K.W., Wang, S., 2003, Peripheral nerve regeneration with sustained release of poly(phosphoester) microencapsulated nerve growth factor within nerve guide conduits. Biomaterials, 24:2405–12.

Zhang, F., Blain, B., Beck, J., Zhang, J., Chen, Z., Chen, Z.W., Lineaweaver, W.C., 2002, Autogenous venous graft with one-stage prepared Schwann cells as a conduit for repair of longseg mental nerve defects. J Reconstr Microsurg, 18:2, 95–300.

Zimmerman, U.P., Schlaepfer, W.W., 1984, Multiple forms of Ca-activated protease from rat brain and muscle, Journal of Biological Chemistry, 259:3210–8.

CURRICULUM VITAE

Name & Surname **:** Yasemin Mısırlı BAYSAL
Place of Birth **:** Bursa
Date of Birth **:** 31.12.1978
Marital Status : Married

Education and Academic Life

High School **:** 1992-1995 Yıldırım Bayazıt High School, Bursa
B. Sc. **:** 1996-2001 Hacettepe University, Chemistry Department
M. Sc. **:** 2001-2004 Hacettepe University, Chemistry Department Biochemistry Division
Ph. D. **:** 2004-2008 Hacettepe University, Chemistry Department Biochemistry Division

Foreign Language:

English

Work Experience

2002- 2008 **:** Research Asistance, Hacettepe University, Chemistry Department.

2008- **:** Customs Laboratory

HSA CALIBRATION CURVE

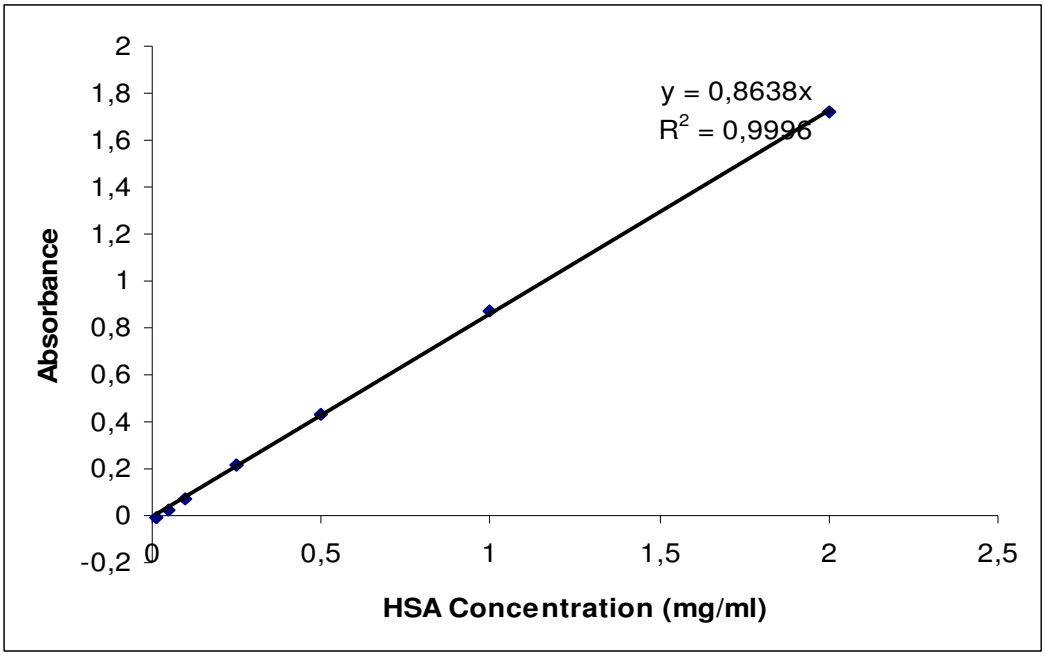

GLUCOSE CALIBRATION CURVE